APPENDIX 6A

SUBCOMPARTMENT DIFFERENTIAL PRESSURE CONSIDERATIONS

Differential pressure analyses were performed for the reactor vessel shield annulus and the drywell head region.

The RPV shield annulus, which is 48.95 ft high and 1.70 ft wide at the top, has the 28 in. recirculation pumps suction lines passing through it. The mass and energy release rates from a postulated recirculation outlet line break constitute the most severe transient in the reactor shield annulus. Therefore, it is selected as the pipe break when analyzing loading of the shield wall and the reactor pressure vessel support skirt for pipe breaks inside the annulus. Estimation of mass and energy release is based on the guidelines set forth in GE's letters to Bechtel; (GB 78-14 dated January 16, 1978 and GB 78-24 dated January 27, 1978) and "Technical Description Annulus Pressurization Load Adequacy Evaluation" (NEDO-24548/78 NED 302).

The subcompartment differential pressure analysis inputs and results presented in this section for the annulus pressurization analysis and the drywell head pressurization analysis are based on the original design basis conditions unless otherwise noted. The blowdown mass and energy release data for the recirculation outlet line break at power uprate conditions has been reanalyzed. The analyses performed for power uprate concluded that the original analyses were conservative and bound power uprate conditions. The original analysis for drywell head pressurization was judged to be overly conservative with respect to power uprate conditions and no reanalysis was performed. Therefore, the design of the shield wall and refueling seal plate is not affected by power uprate.

Recirculation Outlet Line Break

Table 6A-1(a) presents the mass and energy release data estimated by applying the NEDO 24548 method of combining blowdown data calculated from finite and instantaneous break opening time approaches. The blowdown from the supply side is assumed to be released into the annulus due to the break being located in the reactor shield wall penetration. The break is postulated to occur at the nozzle safe end attachment weld to the pipe. The blowdown from the vessel side is vented into the drywell atmosphere. Table 6A-1 (b) provides, as a function of time, the mass flux and areas used for each side of the break. Some physical parameters pertinent to the blowdown rate estimation are noted in the table.

Feedwater Line Break

In addition to the analyses for the recirculation outlet line break in the annulus, similar analyses using the same methodology for blowdown rate estimation are performed for a postulated feedwater line break in the annulus. Table 6A-1(c) presents the mass and energy release rates generated by only applying the very conservative instantaneous break opening time method. The blowdown from the supply side is assumed to enter the annulus due to the location of the postulated break being situated inside the reactor shield wall penetration. The blowdown from the vessel side is released into the drywell. The analysis conservatively assumes that the blowdown from both sides enters the annulus region. The mass flux as a function of time and areas used for each side of the break are presented in Table 6A-1(d). Some pertinent physical parameters are noted in the table.

In addition to the above mentioned lines, there are recirculation inlet lines inside the annulus. Since the recirculation inlet lines are much smaller than the outlet lines, the expected annulus pressurization would not be as severe as for the outlet lines, thus the inlet lines were not analyzed.

Note that the most restricted flow area on the feedwater supply pipe side is the break area itself. Full break area steady state blowdown from this side is conservatively assumed to be reached immediately after the pipe rupture. Note that only the very conservative instantaneous break opening time is used in the generation of Table 6A-1(c) and 6A-1(d) data.

Head Spray Line

In considering the drywell head region, the maximum blowdown rate stems from a break in the RHR head spray line. The blowdown mass and energy release rates for this line are calculated using Moody Critical Flow of 2700 lbm/sec-ft^2 and an enthalpy of 1198 Btu/lbm. Table 6A-2 shows the blowdown schedule for a 6 in. schedule 80S line break with an effective break area of 0.181 ft^2. Since this line could singularly pressurize the drywell head region, it is chosen for analysis in a postulated break.

The annulus pressurization and drywell head pressurization analyses were performed using Bechtel's COPDA computer code. These adjusted pressures are combined with the other appropriate loads (eg, seismic and jet impingement) to develop design loads for the affected structures and components. Subcompartment venting is used to ensure that the differential pressures developed will remain below the structural capability of compartment walls.

BIOLOGICAL SHIELD ANNULUS SUBCOMPARTMENT MODELING PROCEDURES AND ANALYSIS

Biological Shield Annulus

An analysis of the pressure distribution around the reactor pressure vessel after a recirculation outlet line break was performed. The general layout of the shield annulus is shown on Dwgs. C-331, Sh. 1, C-371, Sh. 2, C-1932, Sh. 3, C-1932, Sh. 4, and C-1932, Sh. 5, Figures 6A-1(a) and 6A-1(b). Figure 6A-2 is a schematic of the RPV shield annulus model. The model consists of six major levels. Each level is subdivided into twelve 30° segments to form a total of 72 nodes inside the annulus plus an additional node for the rest of the drywell.

In general, the arrangement of the pipes in the annulus determines the most representative level division, since they constitute the only significant flow restrictions. This 73 pressure node model is considered detailed enough to conservatively predict the maximum pressures on the compartment structure. Therefore, a nodalization sensitivity study is not needed.

For the purpose of determining peak pressure in the reactor vessel shield annulus, all insulation was assumed to move flush against the biological shield wall while still maintaining its original thickness. The volume of the insulation is excluded from the net volume of each subcompartment, and the projected area of the insulation which blocks the venting path is also excluded from the free venting area used in the analysis.

The major vent path to the drywell atmosphere is through the top of the biological shield annulus. Venting through the shield wall is allowed only through the ventilation duct openings at the lower section of the shield wall.

Initial conditions used in this analysis are 15.45 psia, 135°F, and 30 percent relative humidity.

Tables 6A-3 and 6A-4 give the subcompartment volumes, flow areas, L/A ratio, and flow coefficients (including origins) used in the analysis.

The resultant pressure distributions are shown on Figures 6A-3a, 6A-3b, 6A-3c, 6A-3d, 6A-3e, and 6A-3f for the recirculation outlet line break and Figures 6A-3g, 6A-3h, 6A-3i, 6A-3j, 6A-3k, and 6A-3l, for the feedwater line break. The subcompartment pressure existing in each subcompartment at the time of peak differential pressure across the RPV are also shown on these figures. The reactor shield wall is designed for a uniform internal pressure of 70 psig. See Section 3.8.3 for description of the design of the reactor shield wall. COPDA was used to calculate the pressures while the plots were generated using a pre-processor (ABS-PLOT) and TEKPLOT. Additionally, the load forcing functions which include both peak and transient loadings on the RPV and the reactor shield wall are presented on Figures 6A-7 and 6A-8 for the recirculation outlet line break and on Figures 6A-9 and 6A-10 for the feedwater line break. FORCE-GE was used to calculate the forces for the recirculation outlet line break and Bechtel Code NE698 for the feedwater line break while the plots were generated using a pre-processor (ABS-PLOT) and TEKPLOT. This forcing function represents the time-dependent resultant force on the structure and originates from the vector sum of the product of compartment pressure and area for each of the geometry nodes used to represent the surface.

For the recirculation outlet line break the 73 pressure node model is transformed into an 84 geometry node model for calculating the resultant forces. The geometry node model adds another level subdivision but uses the same arc segments. This allows better modeling near the recirculation line nozzle. The locations of the center of each node are given in Table 6A-5. For the feedwater line break the 73 pressure mode model is also used for the force model.

The components of these nodal areas are calculated in the following manner:

$$(A_x)_i = R_i H_i (\text{Sin } \phi_{1_i} - \text{Sin } \phi_{2_i})$$

$$(A_y)_i = R_i H_i (\text{Cos } \phi_{2_i} - \text{Cos } \phi_{1_i})$$

$(A_x)_i$, $(A_y)_i$ = x and y area components for node I

Where

R_i = Radius of the i^{th} geometry node, in.

H_i = Height of the i^{th} geometry node, in.

ϕ_{1_i} = Starting angle (degrees) for i^{th} geometry node

ϕ_{2_i} = Ending angle (degrees) for i^{th} geometry node

For the recirculation outlet line break the resultant areas for each geometry node for the RPV are given in Table 6A-6. For the feedwater line break the resultant areas for each node are given in Table 6A-7. For the bio-shield the node areas are the ratio of the bio-shield radius divided by the RPV radius (12.7917/11.0937 = 1.1531) multiplied by the RPV nodal area.

Therefore, the force generated by a pressure, p_i, acting on a nodal area A_i has the following components:

$$(F_x)_i = P_i(A_x)i$$

$$(F_y)_i = P_i(A_y)i$$

Where

$(F_x)i$, $(F_y)i$ = x and y force components acting on node i

P_i = pressure acting on node i

The compartment pressure transients resulting from a break in the reactor shield annulus generate a nodal force distribution over exposed surfaces. The resultant of this nodal force distribution is presented in Figures 6A-7, 6A-8, 6A-9 and 6A-10. There are no external moments generated by this pressure response. However, any moments would result from the application of the external force distribution to a structural model. This would generate shear stresses (leading to internal moments) due to bending of the elements used to represent the structure as a result of the non-uniform load distribution. Further discussion of this result is contained in Section 3.8.3 where the application of these annulus pressurization results is described in detail.

Blowdown jet loads which include jet impingement and reaction forces against the reactor vessel are also analyzed for reference and comparison. Note that these analyses are based on the very conservative assumptions that the first pipe restraint nearest the nozzle fails. For the feedwater line break, approximately 9.5" pipe center line offset limited by the shield plug opening produces a net break area of 88.53 in², which, consequently, results into a total maximum jet load of 335,600 lbs. against the vessel. These blowdown jet loads are relatively small compared with the peak load contributed by the unbalanced reactor annulus pressurization due to the same breaks.

Subcomponent Annulus Pressurization Loads – Major Project Improvements

Initial Stretch Power Uprate (SPU) & Turbine Retrofit Project (TRP)

An evaluation was performed to analysis the impact on subcompartment annulus pressurization loads for the Stretch Power Uprate (SPU) and Turbine Retrofit Project (TRP) conditions.

A more realistic blowdown mass and energy release profile for RSLB was determined using the RELAP4 MODS computer code. The mass and energy release rates are provided in Table 6A-8. These release rates were calculated using the same physical model as previously described in the licensing analysis section. The results of the RELAP4 analysis yield peak forces on the reactor vessel that are approximately 90% of the original peak forces. Thus, is can be concluded that the original analysis for the reactor annulus differential pressures and resultant reactor vessel and biological shield wall load forcing functions is bounding.

For the FWLB, the blowdown from both sides of the break increases for SPU and TRP. As stated previously with regards to the FWLB, only the supply side blowdown enters the annulus region. Using the approach, the supply side blowdown for SPU/TRP is less than the total blowdown used in the original analysis; therefore, the previously analyzed loads were bounding.

Maximum Extended Lad Line Limit Analysis (MELLLA)

An evaluation was performed to analysis the impact on subcompartment annulus pressurization loads for operation in the Maximum Extended Load Line Limit Analysis (MELLLA) reactor operating domain.

A more realistic blowdown mass and energy release profile for RSLB was determined using the GE code LAMB for the AP load analysis. The LAMB code considers the pipe break separation time history, but ignores the fluid inertia effect, providing conservative results. This code analysis was accepted by the NRC during the licensing application. LAMB results at the minimum pump speed condition are bounded by the Susquehanna original analysis.

For the FWLB, the blowdown, as indicated by the flux of steam flashed from the mass blowdown, is bounded by that at the rated MELLLA power condition.

Extended Power Uprate (EPU)

An evaluation was performed to analyze the impact on subcompartment annulus pressurization loads with an increase in reactor thermal power at Extended Power Uprate (EPU) conditions.

For the RRLB, the analysis and conclusions reached for MELLLA domain remain valid.

For the FWLB, the blowdown from both side of the break increases for SPU and TRP. As stated previously with regards to the FWLB, only the supply side blowdown enters the annulus region. Using this approach, the supply side blowdown for SPU/TRP is less than the total blowdown used in the original analysis; therefore, the original analyzed loads are bounding.

DRYWELL HEAD REGION SUBCOMPARTMENT ANALYSIS

The design basis pressure differential between the drywell head and containment region is a structural requirement of the drywell head. A pressure analysis of the drywell head region for a postulated head spray line break was performed.

Figure 6A-4 illustrates the basic arrangement of the head region. Venting from the head region is accomplished through ventilation openings as shown on Figure 6A-4. These vent openings provide a total of 16.75 sq. ft. vent area with an equivalent orifice (slightly rounded) discharge coefficient of 0.67 to relieve pressure build-up caused by the postulated break.

Figure 6A-5 is the schematic flow diagram with vent flow areas and discharge coefficient used in the drywell head venting analysis.

To determine peak pressure in the drywell head, all insulation was assumed to remain in place. Initial conditions of 15.4 psia, 135°F, and 20 percent relative humidity were used in this analysis.

The pressure transient of this analysis is presented on Figure°6A-6. It can be seen that the maximum pressure in the drywell head region is 23.2 psia and occurs 0.83 seconds after the head spray line break. Considering the containment pressure to be atmospheric (no drywell air displaced into the containment), a drywell head to containment pressure differential of 8.5 psid is obtained. This pressure differential is well below the design pressure differential of 16.0 psid.

TABLE 6A-1(a)

REACTOR PRIMARY SYSTEM BLOWDOWN FLOW RATES AND FLUID ENTHALPY - RECIRCULATION OUTLET LINE BREAK

Time (sec)	Mass Flow (lbm/sec)	Enthalpy (Btu/lbm)
0.000	0.0000	0.000
2.5500-03	1.3400+03	527.9
3.9000-03	2.6750+03	527.9
4.9600-03	4.0100+03	527.9
5.8600-03	5.3500+03	527.9
7.3700-03	8.0200+03	527.9
9.2400-03	1.2025+04	527.9
1.1800-02	1.9285+04	527.9
1.3800-02	2.6560+04	527.9
1.5800-02	3.2355+04	527.9
1.8000-02	4.5975+04	527.9
2.0800-02	4.5975+04	527.9
2.0800-02	2.2400+04	527.9
2.1800-02	2.4130+04	527.9
2.2800-02	2.5840+04	527.9
2.3800-02	2.7520+04	527.9
2.5800-02	3.0780+04	527.9
2.7800-02	3.3880+04	527.9
3.0800-02	3.8170+04	527.9
3.5800-02	4.4220+04	527.9
3.7000-02	4.5975+04	527.9
4.1400-01	4.5975+04	527.9
4.1400-01	3.4370+04	527.9
1.0000+00	3.4370+04	527.9

TABLE 6A-1(b)

RECIRC. OUTLET LINE BREAK BLOWDOWN MASS FLUX TIME HISTORY

Time (seconds)	Mass Flux (lbm/sec/ft²)	Effective Break Area (ft²)
Vessel Side		
0.00255	21200	0.0316
0.00496	21200	0.0964
0.00737	21200	0.1892
0.01180	21200	0.4548
0.01580	21200	0.7631
0.02080	21200	1.0843
0.02081	8410	1.3317
0.02180	8410	1.4346
0.02380	8410	1.6361
0.02780	8410	2.0142
0.03580	8410	2.6290
0.03700	8410	2.7333
0.41400	8410	3.6440
0.41410	8410	3.6440
1.0	8410	3.6440
Pump Side		
0.00255	21200	0.0316
0.00496	21200	0.0964
0.00737	21200	0.1892
0.01180	21200	0.4548
0.01580	21200	0.7631
0.02080	21200	1.0843
0.02081	8410	1.3317
0.02180	8410	1.4346
0.02380	8410	1.6361
0.02780	8410	2.0142
0.03580	8410	2.6290
0.03700	8410	2.7333
0.41400	8410	1.8220
0.41410	8410	0.4420
1.0	8410	0.4420

NOTE: Listed below are pertinent physical parameters used in the blowdown estimation.

$A = 3.644\ ft^2$	Minimum cross-sectional area between vessel and break
$D = 2.154\ ft$	Pipe I.D. at the break location
$ho = 527.85\ Btu/Lbm$	Vessel enthalpy
$Li = 2.917\ ft$	Inventory length
$Po = 1031.2\ psia$	Vessel pressure
$Psat = 908\ psia$	Saturation pressure
$V = 0.02127\ ft^3/lbm$	Specific volume of the fluid initially in the pipe
$Vi = 135\ ft^3$	Inventory volume

TABLE 6A-1(c)

REACTOR PRIMARY SYSTEM BLOWDOWN FLOW RATES AND FLUID ENTHALPY - FEEDWATER LINE BREAK

Time (sec)	Mass Flow (lbm/sec)	Enthalpy (Btu/lbm)
0	0	361.1
0.0001	21830	361.1
0.0207	21830	361.1
0.0208	20075	361.1
1.0	20075	361.1

TABLE 6A-1(d)

FEEDWATER LINE BREAK BLOWDOWN MASS FLUX TIME HISTORY

Vessel Side:

Time (sec)	Mass Flux (lbm/sec/Ft^2)	Effective Break Area (Ft^2)
0.0001	20625	0.3528
0.0207	20625	0.3528
0.0208	20625	0.2679
1.0	20625	0.2679
Supply Pipe Side (1) (3):		
0.0001	20625	0.7055
1.0	20625	0.7055

NOTES:

(1) The most restricted flow area on the feedwater supply pipe side is the break area itself. Full break area steady state blowdown from this side is conservatively assumed to be reached immediately after the pipe rupture.

(2) Listed below are some pertinent physical parameters used in the blowdown estimation:

A_L = 0.7055 ft^2	Minimum cross-sectional area - supply pipe side
D = 0.9478	Pipe I.D. at the break location
ho = 361.1 Btu/Lbm	FW enthalpy
Po = 1053 PSIA	Vessel pressure
Psat = 213 PSIA	Saturation pressure
v = 0.01846 ft^3/Lbm	Specific volume of the feedwater
vi = 2.79 ft^3	Inventory volume

(3) Annulus pressurization is based on blowdown flow from the supply side only. Based on the break location, flow from the vessel side is expected to exit directly to the drywell.

TABLE 6A-2

HEAD SPRAY LINE BREAK(1)

Time (sec)	Steam Flow (lbm/sec)	Steam Enthalpy (Btu/lbm)
0.0	490	1198
20.0	490	1198

(1) Head spray line break is based on 6 in. Schedule 80S pipe with Moody Blowdown corresponding to 2700 lbm/sec-sq ft. Overall containment response is that of a "small break accident".

TABLE 6A-3

SUSQUEHANNA-COMPARTMENT VOLUMES USED IN REACTOR VESSEL SHIELD ANNULUS SUBCOMPARTMENT ANALYSIS

COMPARTMENT NO.	DESIGNATION	VOLUME, ft^3
1	V1	54
2	V2	54
3	V3	54
4	V4	54
5	V5	54
6	V6	54
7	V7	54
8	V8	54
9	V9	54
10	V10	54
11	V11	54
12	V12	54
13	V13	69
14	V14	76
15	V15	75
16	V16	76
17	V17	76
18	V18	69
19	V19	69
20	V20	76
21	V21	75
22	V22	76
23	V23	76
24	V24	69
25	V25	59
26	V26	57
27	V27	57
28	V28	57
29	V29	57
30	V30	57
31	V31	57
32	V32	57
33	V33	57
34	V34	57
35	V35	57
36	V36	59
37	V37	60
38	V38	58
39	V39	60
40	V40	76
41	V41	58

TABLE 6A-3

SUSQUEHANNA-COMPARTMENT VOLUMES USED IN REACTOR VESSEL SHIELD ANNULUS SUBCOMPARTMENT ANALYSIS

COMPARTMENT NO.	DESIGNATION	VOLUME, ft^3
42	V42	60
43	V43	76
44	V44	58
45	V45	60
46	V46	76
47	V47	58
48	V48	60
49	V49	77
50	V50	71
51	V51	73
52	V52	77
53	V53	75
54	V54	77
55	V55	77
56	V56	74
57	V57	77
58	V58	73
59	V59	71
60	V60	77
61	V61	34
62	V62	34
63	V63	34
64	V64	34
65	V65	34
66	V66	34
67	V67	34
68	V68	34
69	V69	34
70	V70	34
71	V71	34
72	V72	34
73	V73	235200

TABLE 6A-4 (1 of 4)

SUSQUEHANNA - FLOW AREA AND COEFFICIENTS USED IN REACTOR VESSEL SHIELD ANNULUS SUBCOMPARTMENT ANALYSIS

Flow Paths	Flow Area (ft^2)	K Factor	Description	L/A (ft^{-1})	Flow Coefficient
1-2,1-12, 2-3,3-4, 4-5,5-6, 6-7,7-8, 8-9,9-10, 10-11,11-12	10	0.13 1.0	30° Turn Final Expansion	0.62	0.94
1-13,2-14, 3-15,4-16, 5-17,6-18, 7-19,8-20, 9-21,10-22, 11-23,12-24	8.5	0.05 1.0	Friction Final Expansion	1.01	0.97
2-73,3-73, 5-73,6-73, 8-73,9-73, 11-73,12-73	2	0.42 1.0	Contraction Final Expansion	0.73	0.83
13-24, 18-19	9.5	0.13 1.12 1.0	30° Turn Around Pipe Final Expansion	0.54	0.66
13-14,15-16, 16-17,17-18, 19-20,20-21, 22-23,23-24	13	0.13 0.1 1.0	30° Turn Around Pipe Final Expansion	0.43	0.9
14-15, 21-22	12	0.1 0.1 0.13 1.0	Around Pipe Around Instrument Pipe 30° Turn Final Expansion	0.43	0.86
13-25,18-30, 19-31,24-36	4.5	1.35 0.28 1.0	Around Pipe Around Pipe Final Expansion	1.57	0.61
14-26,16-28, 17-29,20-32, 22-34,23-35,	5.5	0.28 0.28 1.0	Around Pipe Around Pipe Final Expansion	1.17	0.8
15-27, 21-33	4.5	0.28 0.28 0.31 1.0	Around Pipe Around Pipe Around Pipe Final Expansion	1.31	0.73

TABLE 6A-4 (Continued) (2 of 4)

Flow Paths	Flow Area (ft^2)	K Factor	Description	L/A (ft^{-1})	Flow Coefficient
25-36,		0.13	30° Turn		
30-31	11	1.0	Final Expansion	0.55	0.94
25-26,26-27,					
27-28,28-29,					
29-30,31-32,		0.13	30° Turn		
32-33,33-34,		0.16	Around Pipe		
34-35,35-36,	9.5	1.0	Final Expansion	0.58	0.88
25-37,26-38,					
27-39,28-40,					
29-41,30-42,					
31-43,32-44,					
33-45,34-46,		0.07	Friction		
35-47,36-48	8.5	1.0	Final Expansion	0.92	0.96
		0.13	30° Turn		
37-48,38-39		0.01	Around Instrument Pipe		
41-42,45-46	10.5	1.0	Final Expansion	0.55	0.93
		0.13	30° Turn		
37-38,40-41,		0.16	Around Pipe		
44-45,47-48	9.5	1.0	Final Expansion	0.57	0.88
39-40,42-43,		0.13	30° Turn		
43-44,46-47	11	1.0	Final Expansion	0.55	0.94
		0.01	Around Instrument Pipe		
37-49,		0.07	Friction		
48-60	8	1.0	Final Expansion	1.07	0.96
38-50,41-53,		1.11	Around Pipe		
44-56,47-59	6	1.0	Final Expansion	1.14	0.68
39-51,42-54,		0.08	Around Instrument Pipe		
45-57	8	1.0	Final Expansion	1.07	0.96
40-52,43-55		0.07	Around Pipe		
46-58	8.5	1.0	Final Expansion	1.06	0.96
		0.13	30° Turn		
		0.15	Around Pipe		
49-50		0.15	Around Pipe		
59-60	11.5	1.0	Final Expansion	0.46	0.83

TABLE 6A-4 (Continued) (3 of 4)

Flow Paths	Flow Area (ft^2)	K Factor	Description	L/A (ft^{-1})	Flow Coefficient
		0.125	30° Turn		
		0.01	Around Instrument Pipe		
49-60	14	1.0	Final Expansion	0.42	0.93
		0.13	30° Turn		
		0.01	Around Instrument Pipe		
		0.47	Around Pipe		
50-51	10.5	1.0	Final Expansion	0.48	0.78
		0.13	30° Turn		
51-52,52-53,		0.15	Around Pipe		
56-57	13	1.0	Final Expansion	0.44	0.88
		0.13	30° Turn		
		0.01	Around		
		0.15	Around		
53-54,57-58	12.5	1.0	Final Expansion	0.45	0.88
		0.13	30° Turn		
54-55	14.5	1.0	Final Expansion	0.42	0.94
		0.13	30° Turn		
		0.15	Around Pipe		
		0.12	Around CRD		
		0.15	Around Pipe		
55-56	10.5	1.0	Final Expansion	0.5	0.8
		0.13	30° Turn		
		0.47	Around Pipe		
58-59	11	1.0	Final Expansion	0.47	0.79
49-61,52-64,					
53-65,55-67,		0.49	Around Pipe		
57-69	6.5	1.0	Final Expansion	0.96	0.81
		0.49	Around Pipe		
54-66,		0.08	Around Instrument Pipe		
60-72	6	1.0	Final Expansion	1.0	0.79
		0.49	Around Pipe		
		0.17	Around CRD		
56-68	5.5	1.0	Final Expansion	1.07	0.77
61-62,63-64		0.11	30° Turn		
67-68,69-70		0.96	Around Pipe		
71-72	5	1.0	Final Expansion	1.03	0.69

TABLE 6A-4 (Continued) (4 of 4)

Flow Paths	Flow Area (ft^2)	K Factor	Description	L/A (ft^{-1})	Flow Coefficient
61-72,62-63					
64,65,66-67		0.11	30° Turn		
68-69,70-71	6.5	1.0	Final Expansion	0.9	0.94
		0.11	30° Turn		
		0.96	Around Pipe		
65-66,		0.1	Around Instrument Pipe		
71-62	4.5	1.0	Final Expansion	1.1	0.67
61-73,63-73					
64-73,66-73					
67-73,69-73		0.12	Contraction		
70-73,72-73	6	1.0	Final Expansion	0.28	0.94
62-73,65-73		0.05	Contraction		
68-73,71-73	7.5	1.0	Final Expansion	0.28	0.97

TABLE 6A-5

Geometry Node Locations

Node Numbers	Elevation
1 - 12	733' - 4-13/16"
13 - 24	740' - 7"
25 - 36	745' - 9-1/2"
37 - 48	751' - 4-7/8"
49 - 60	759' - 4-5/8"
61 - 72	766' - 2-1/4"
73 - 84	773' - 10-1/2"

Node Angles	Node Numbers
345°	1, 13, 25, 37, 49, 61, 73
315°	2, 14, 26, 38, 50, 62, 74
285°	3, 15, 27, 39, 51, 63, 75
255°	4, 16, 28, 40, 52, 64, 76
225°	5, 17, 29, 41, 53, 65, 77
195°	6, 18, 30, 42, 54, 66, 78
165°	7, 19, 31, 43, 55, 67, 79
135°	8, 20, 32, 44, 56, 68, 80
105°	9, 21, 33, 45, 57, 69, 81
75°	10, 22, 34, 46, 58, 70, 82
45°	11, 23, 35, 47, 59, 71, 83
15°	12, 24, 36, 48, 60, 72, 84

Note: Elevations and node angles are for center of geometry nodes.

TABLE 6A-6

RPV GEOMETRY NODE AREAS FOR RECIRCULATION OUTLET LINE BREAK

Geometry Node Number	Area (x) (inch^2) based on RPV (inside) radius	Area (y) (inch^2) based on RPV (inside) radius
1	5741	1541
2	4209	4209
3	1541	5749
4	1541	5749
5	4209	4209
6	5749	1540
7	5749	1541
8	4209	4209
9	1541	5749
10	1541	5749
11	4209	4209
12	5749	1541
13	5724	1534
14	4191	4191
15	1534	5724
16	1534	5724
17	4191	4190
18	5724	1534
19	5724	1534
20	4190	4191
21	1534	5724
22	1534	5724
23	4190	4190
24	5724	1534
25	2596	696

TABLE 6A-6

RPV GEOMETRY NODE AREAS FOR RECIRCULATION OUTLET LINE BREAK

Geometry Node Number	Area (x) (inch^2) based on RPV (inside) radius	Area (y) (inch^2) based on RPV (inside) radius
26	1900	1900
27	696	2596
28	696	2596
29	1900	1870
30	2596	690
31	2596	690
32	1900	1900
33	696	2596
34	696	2596
35	1900	1900
36	2596	696
37	6373	1708
38	4666	4666
39	1708	6373
40	1708	6373
41	4665	4665
42	6373	1708
43	6373	1708
44	4666	4666

TABLE 6A-7

RPV GEOMETRY MODE AREAS FOR FEEDWATER LINE BREAK

Geometry Mode Number	Area (x) (inch^2) based on RPV (inside) radius	Area (y) (inch^2) based on RPV (inside) radius
1	5749	1541
2	4209	4209
3	1541	5749
4	1541	5749
5	4209	4209
6	5749	1541
7	5749	1541
8	4209	4209
9	1541	5749
10	1541	5749
11	4209	4209
12	5749	1541
13	8320	2229
14	6091	6091
15	2229	8320
16	2229	8320
17	6091	6091
18	8320	2229
19	8320	2229
20	6091	6091
21	2229	8320
22	2229	8320
23	6091	6091
24	8320	2229
25	6373	1708

TABLE 6A-7

RPV GEOMETRY MODE AREAS FOR FEEDWATER LINE BREAK

Geometry Mode Number	Area (x) (inch^2) based on RPV (inside) radius	Area (y) (inch^2) based on RPV (inside) radius
26	4666	4666
27	1708	6373
28	1708	6373
29	4666	4666
30	6373	1708
31	6373	1708
32	4666	4666
33	1708	6373
34	1708	6373
35	4666	4666
36	6373	1708
37	6373	1708
38	4666	4666
39	1708	6373
40	1708	6373
41	4666	4666
42	6373	1708
43	6373	1708
44	4666	4666

TABLE 6A-8

REACTOR PRIMARY SYSTEM BLOWDOWN FLOW RATES AND FLUID ENTHALPY - RECIRCULATION OUTLET LINE BREAK

POWER UPRATE VALUES

Time (sec)	Mass Flow (lbm/sec)	Enthalpy (Btu/lbm)
0	0.00	0.00
1.000-03	3.2400+02	526.8
2.170-03	9.9100+02	526.8
2.180-03	9.9800+02	526.8
4.600-03	3.3750+03	526.8
6.900-03	6.8700+03	526.8
8.600-03	1.0245+04	526.8
1.010-02	1.3741+04	526.8
1.260-02	2.0370+04	526.8
1.510-02	2.7481+04	526.8
1.760-02	3.4834+04	526.8
2.010-02	4.1945+04	526.8
2.260-02	4.8936+04	526.8
2.363-02	5.1640+04	526.8
2.771-02	5.1640+04	526.8
2.772-02	2.7786+04	526.8
3.010-02	3.0200+04	526.8
3.260-02	3.2523+04	526.8
3.510-02	3.4576+04	526.8
3.760-02	3.6359+04	526.8
4.010-02	3.7764+04	526.8
4.260-02	3.8898+04	526.8
4.780-02	4.0141+04	526.8
1.000+00	4.0141+04	526.8

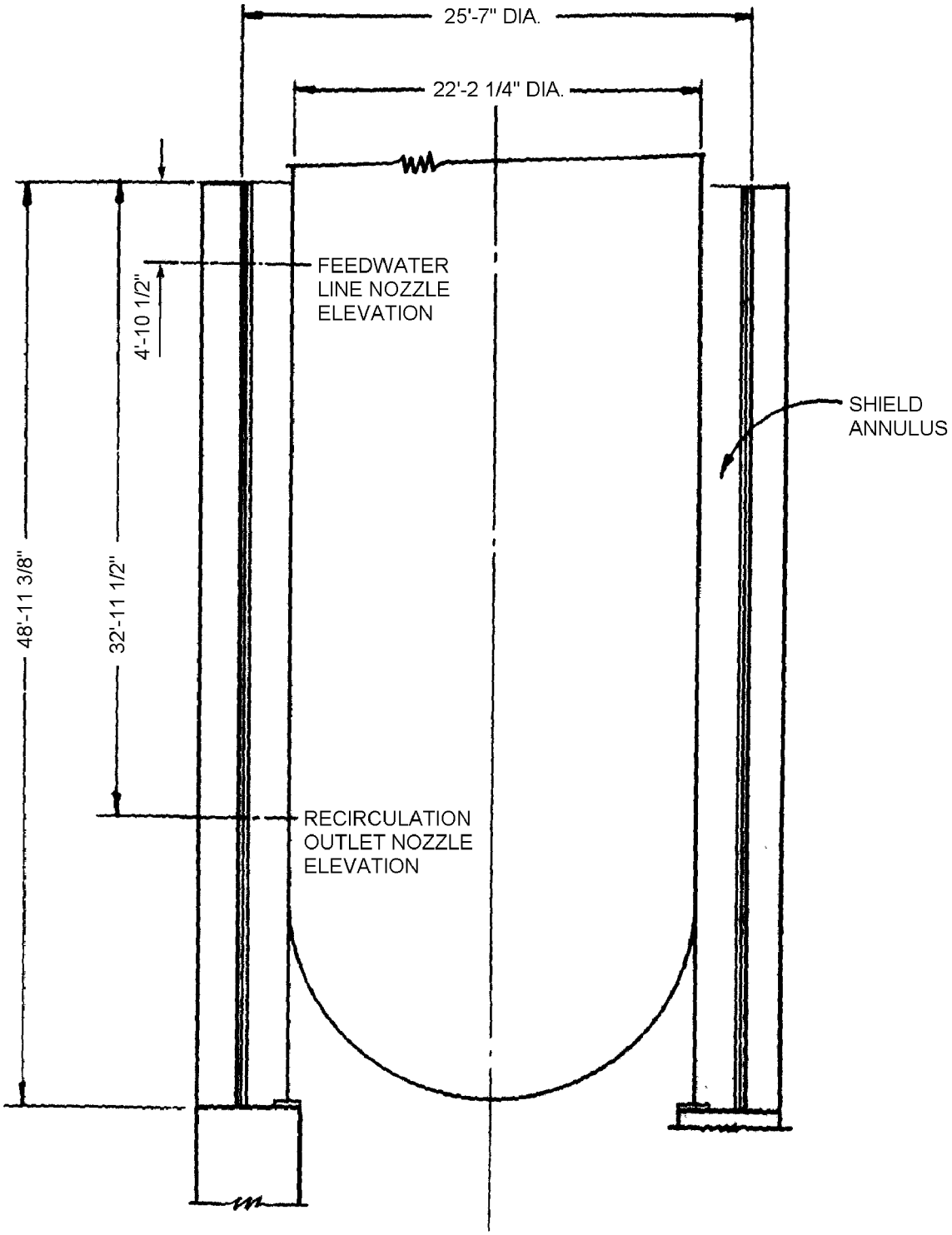

FSAR REV.65

SUSQUEHANNA STEAM ELECTRIC STATION
UNITS 1 & 2
FINAL SAFETY ANALYSIS REPORT

REACTOR SHIELD ANNULUS
ARRANGEMENT

FIGURE 6A-1A, Rev. 55

AutoCAD: Figure Fsar 6A_1A.dwg

Security-Related Information
Figure Withheld Under 10 CFR 2.390

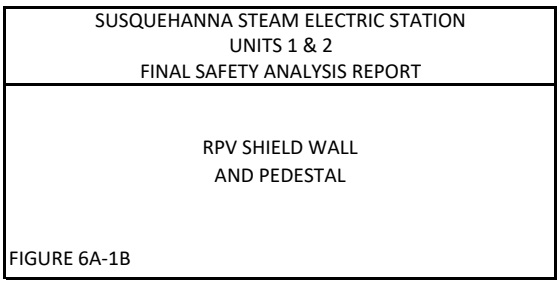

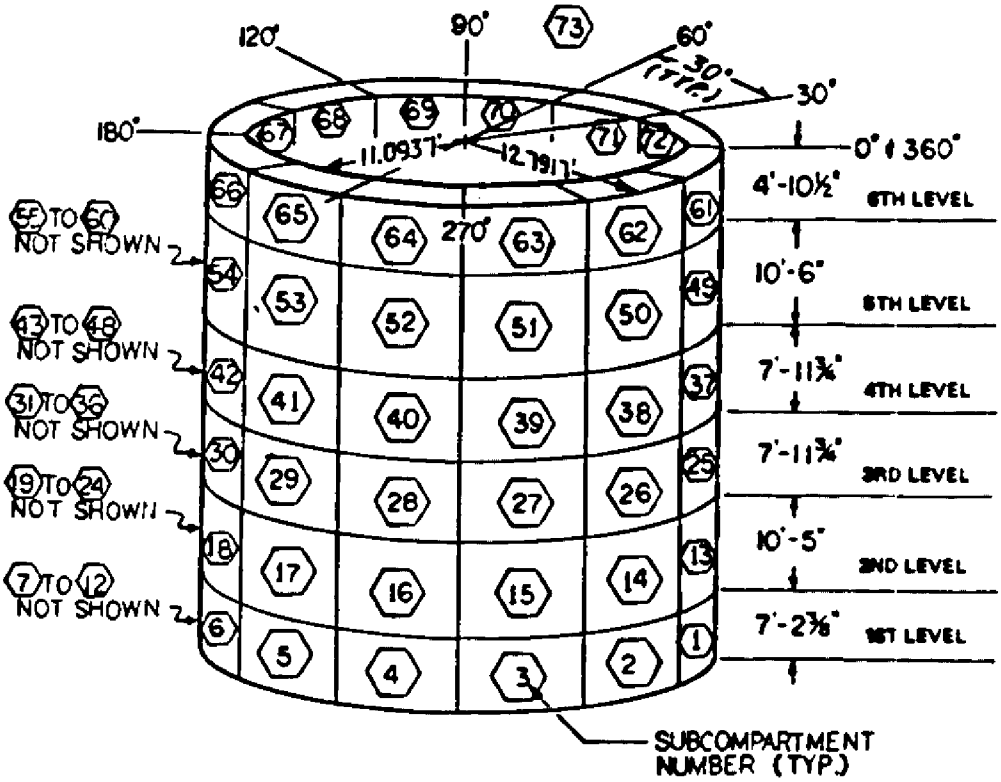

FEEDWATER PIPE BREAK IN SUBCOMPARTMENTS 57, 58, 69 AND 70

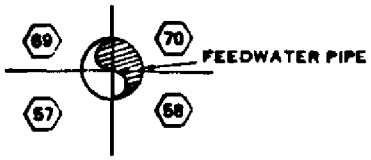

RECIRCULATION OUTLET PIPE BREAK IN SUBCOMPARTMENT 13 AND 14

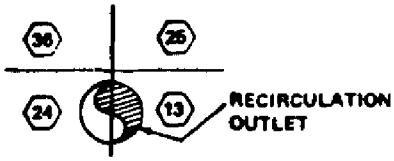

FSAR REV.65

SUSQUEHANNA STEAM ELECTRIC STATION
UNITS 1 & 2
FINAL SAFETY ANALYSIS REPORT

RPV SHIELD ANNULUS
SUBCOMPARTMENT
MODEL SCHEMATIC

FIGURE 6A-2, Rev. 47

AutoCAD: Figure Fsar 6A_2.dwg

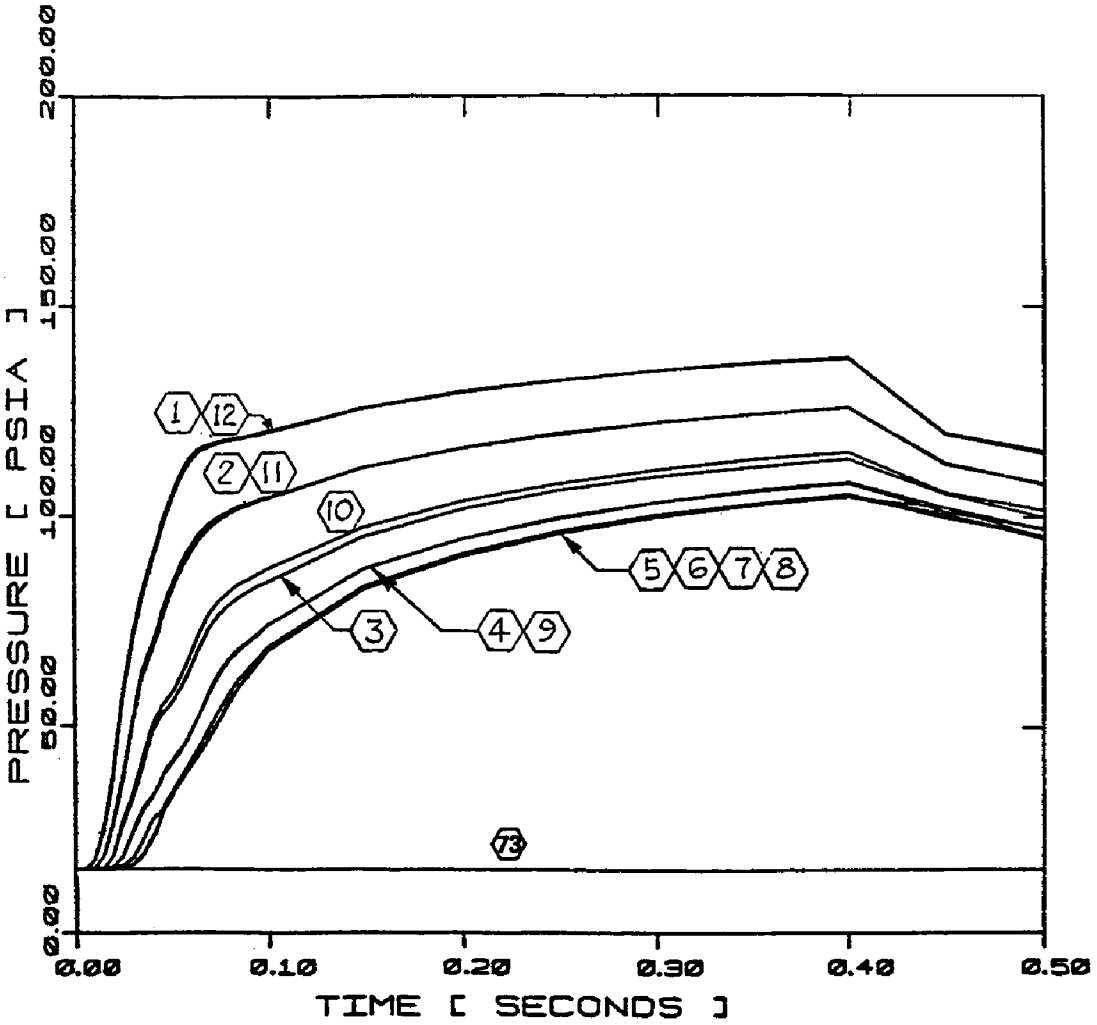

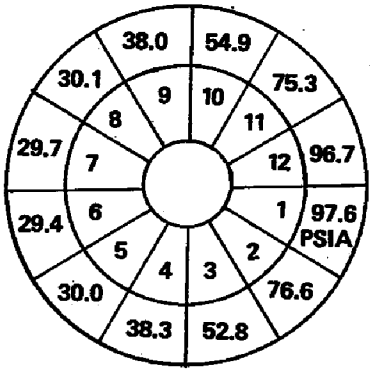

1ST LEVEL

THE ABOVE SPACIAL PRESSURE DISTRIBUTION OCCURS AT 0.046 SEC PRODUCING THE MAXIMUM DIFFERENTIAL PRESSURE ACROSS THE VESSEL

FSAR REV.65

SUSQUEHANNA STEAM ELECTRIC STATION
UNITS 1 & 2
FINAL SAFETY ANALYSIS REPORT

PRESSURE TRANSIENT IN
SHIELD ANNULUS FOLLOWING
A RECIRC. LINE BREAK AT
THE NOZZLE SAFE END

FIGURE 6A-3A, Rev. 47

AutoCAD: Figure Fsar 6A_3A.dwg

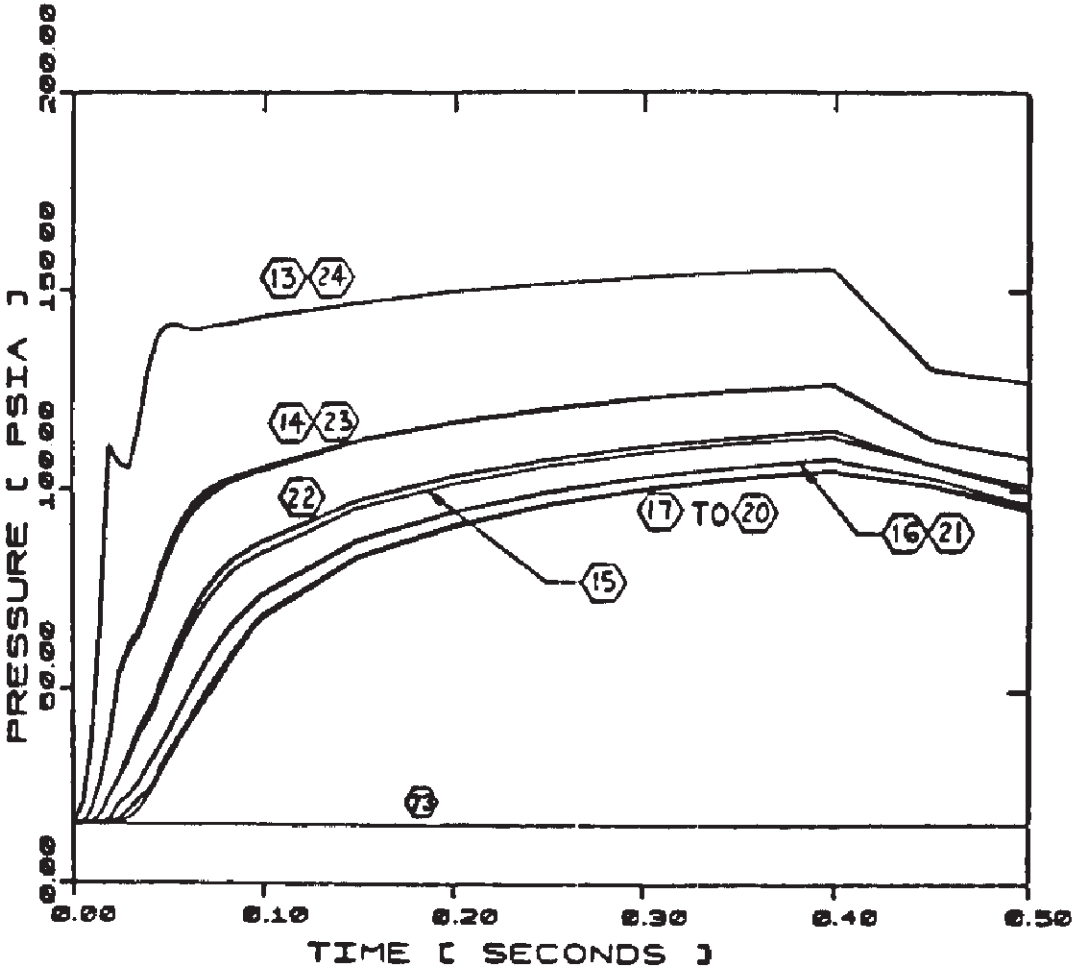

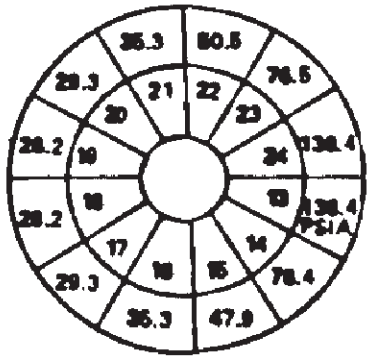

2ND LEVEL

THE ABOVE SPACIAL PRESSURE DISTRIBUTION OCCURS AT 0.046 SEC PRODUCING THE MAXIMUM DIFFERENTIAL PRESSURE ACROSS THE VESSELL

FSAR REV.65

SUSQUEHANNA STEAM ELECTRIC STATION
UNITS 1 & 2
FINAL SAFETY ANALYSIS REPORT

PRESSURE TRANSIENT IN SHIELD ANNULUS FOLLOWING A RECIRC. LINE BREAK AT THE NOZZLE SAFE END

FIGURE 6A-3B, Rev. 47

AutoCAD: Figure Fsar 6A_3B.dwg

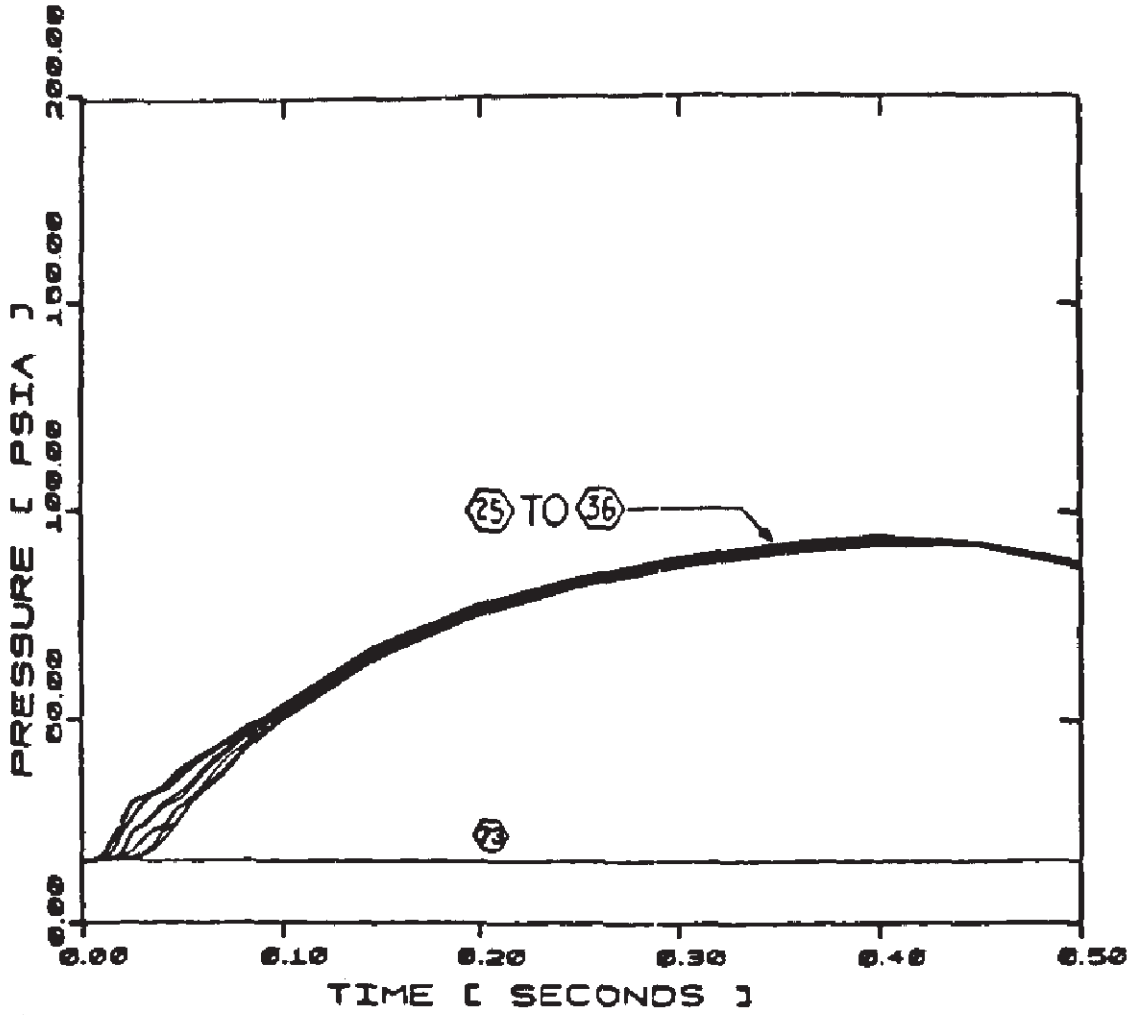

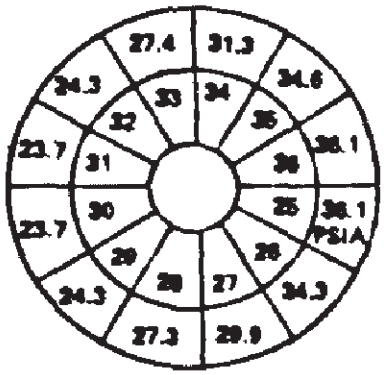

3RD LEVEL

THE ABOVE SPACIAL PRESSURE DISTRIBUTION OCCURS AT 0.046 SEC PRODUCING THE MAXIMUM DIFFERENTIAL PRESSURE ACROSS THE VESSEL

FSAR REV.65

SUSQUEHANNA STEAM ELECTRIC STATION
UNITS 1 & 2
FINAL SAFETY ANALYSIS REPORT

PRESSURE TRANSIENT IN SHIELD ANNULUS FOLLOWING A RECIRC. LINE BREAK AT THE NOZZLE SAFE END

FIGURE 6A-3C, Rev. 47

AutoCAD: Figure Fsar 6A_3C.dwg

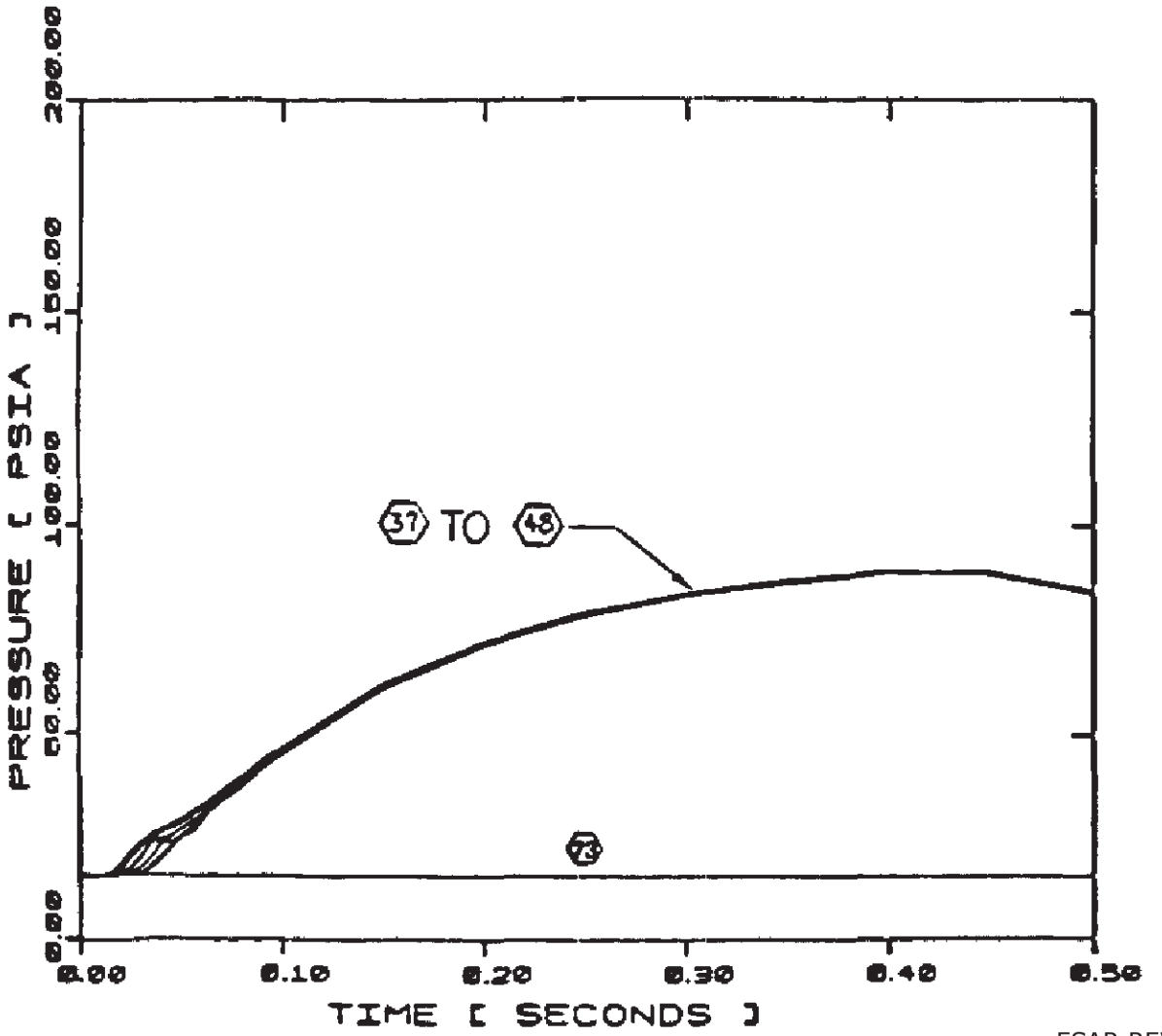

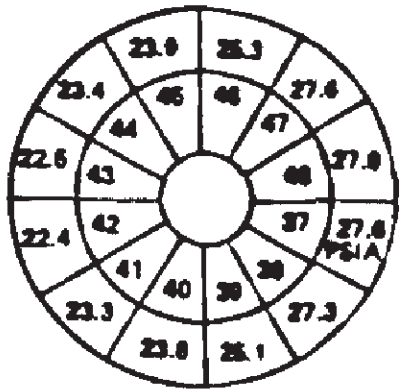

4TH LEVEL

THE ABOVE SPACIAL PRESSURE DISTRIBUTION OCCURS AT 0.048 SEC PRODUCING THE MAXIMUM DIFFERENTIAL PRESSURE ACROSS THE VESSEL

FSAR REV.65

SUSQUEHANNA STEAM ELECTRIC STATION
UNITS 1 & 2
FINAL SAFETY ANALYSIS REPORT

PRESSURE TRANSIENT IN SHIELD ANNULUS FOLLOWING A RECIRC. LINE BREAK AT THE NOZZLE SAFE END

FIGURE 6A-3D, Rev. 47

AutoCAD: Figure Fsar 6A_3D.dwg

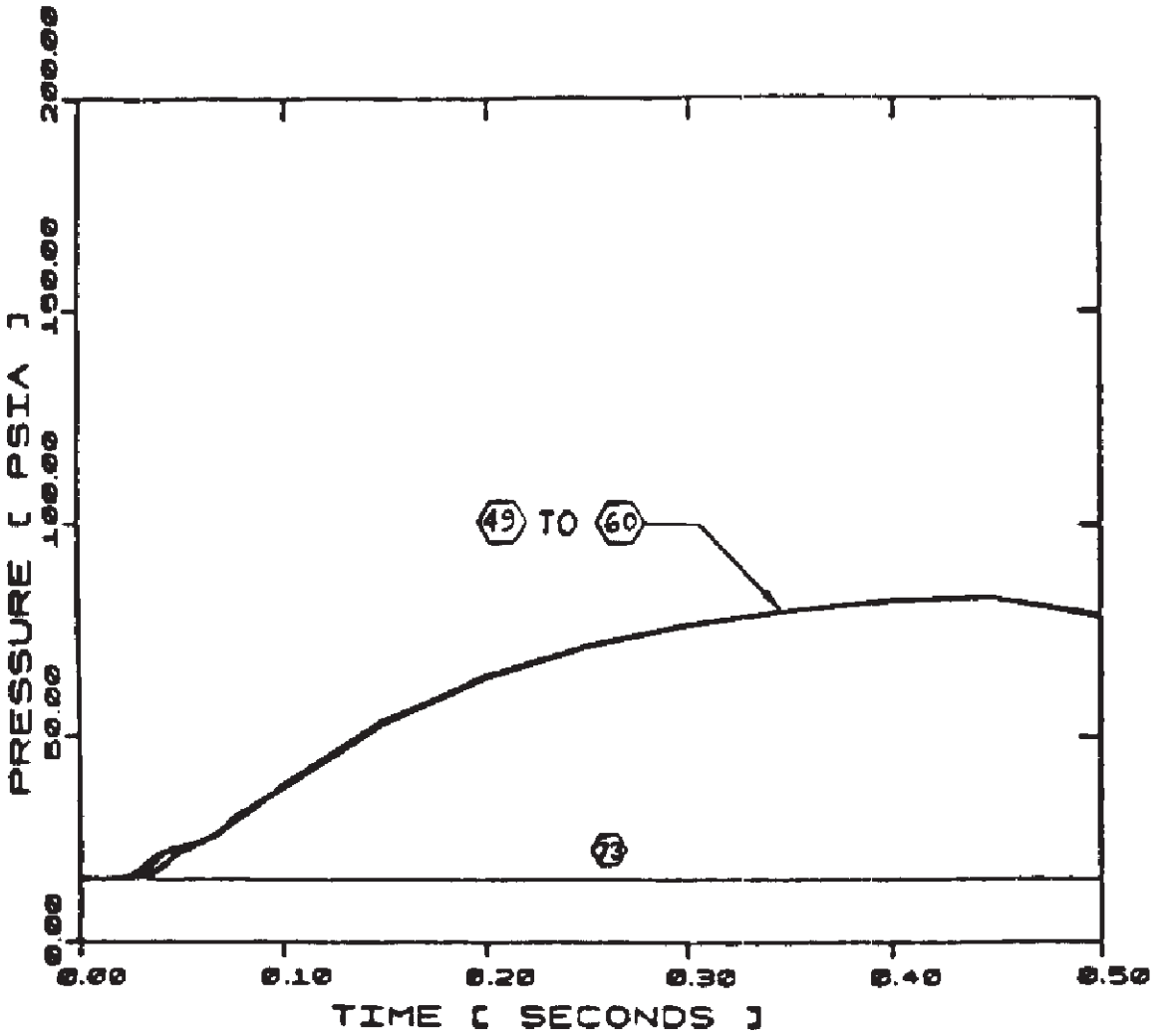

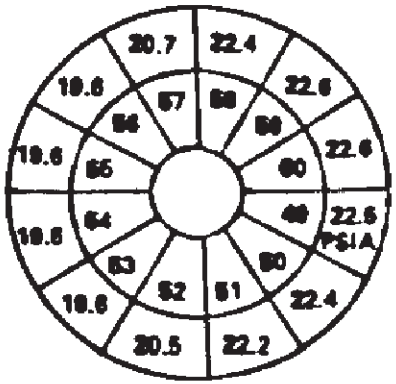

6TH LEVEL

THE ABOVE SPACIAL PRESSURE DISTRIBUTION OCCURS AT 0.040 SEC PRODUCING THE MAXIMUM DIFFERENTIAL PRESSURE ACROSS THE VESSEL

FSAR REV.65

SUSQUEHANNA STEAM ELECTRIC STATION
UNITS 1 & 2
FINAL SAFETY ANALYSIS REPORT

PRESSURE TRANSIENT IN SHIELD ANNULUS FOLLOWING A RECIRC. LINE BREAK AT THE NOZZLE SAFE END

FIGURE 6A-3E, Rev. 47

AutoCAD: Figure Fsar 6A_3E.dwg

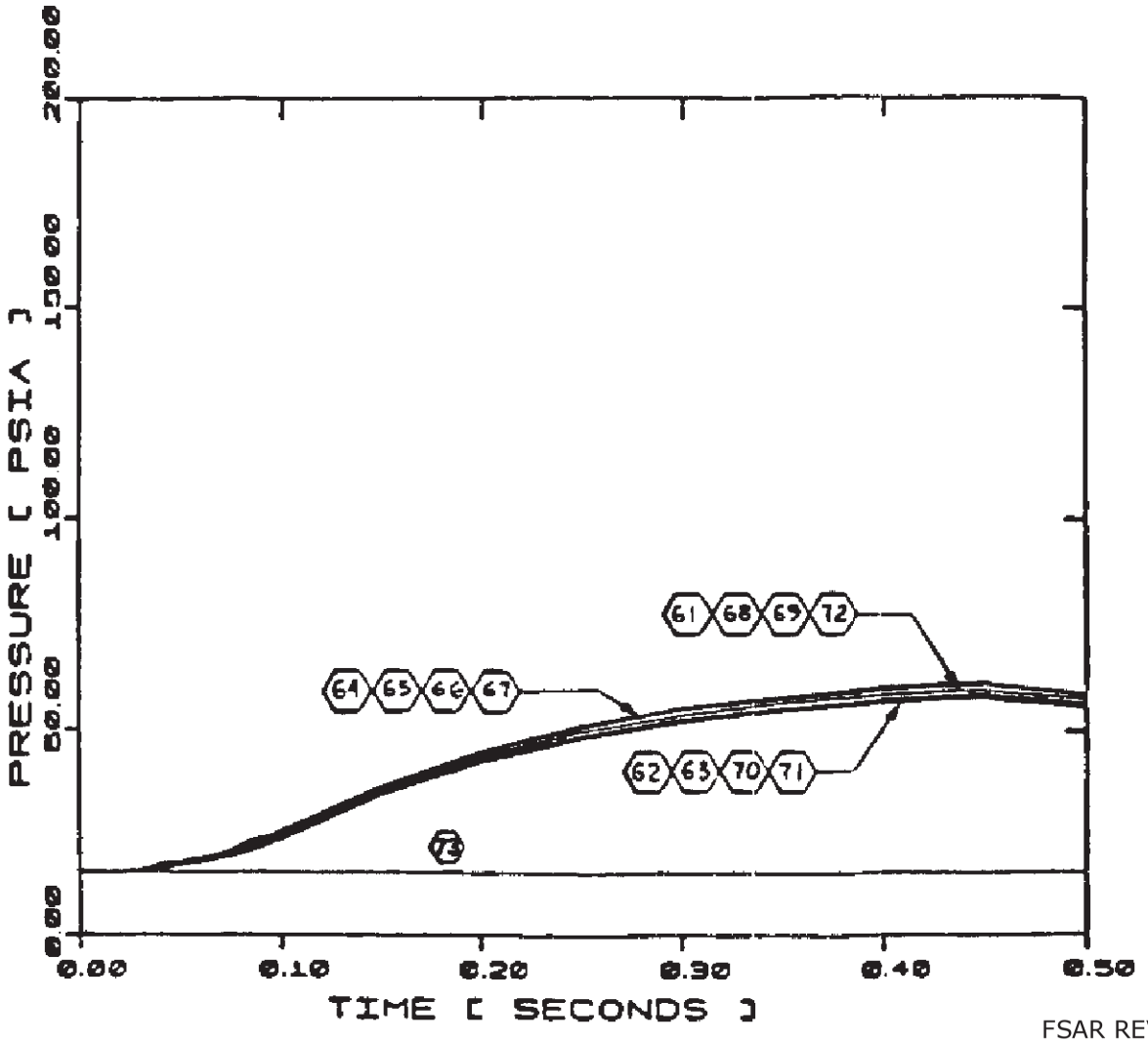

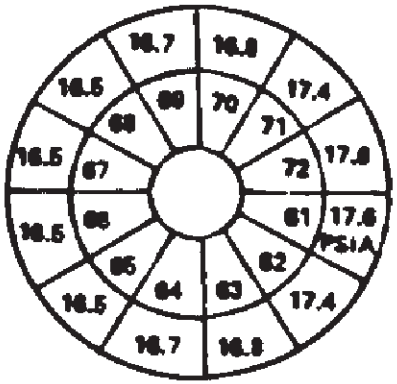

6TH LEVEL

THE ABOVE SPACIAL PRESSURE DISTRIBUTION OCCURS AT 0.048 SEC PRODUCING THE MAXIMUM DIFFERENTIAL PRESSURE ACROSS THE VESSEL.

FSAR REV.65

SUSQUEHANNA STEAM ELECTRIC STATION
UNITS 1 & 2
FINAL SAFETY ANALYSIS REPORT

PRESSURE TRANSIENT IN SHIELD ANNULUS FOLLOWING A RECIRC. LINE BREAK AT THE NOZZLE SAFE END

FIGURE 6A-3F, Rev. 47

AutoCAD: Figure Fsar 6A_3F.dwg

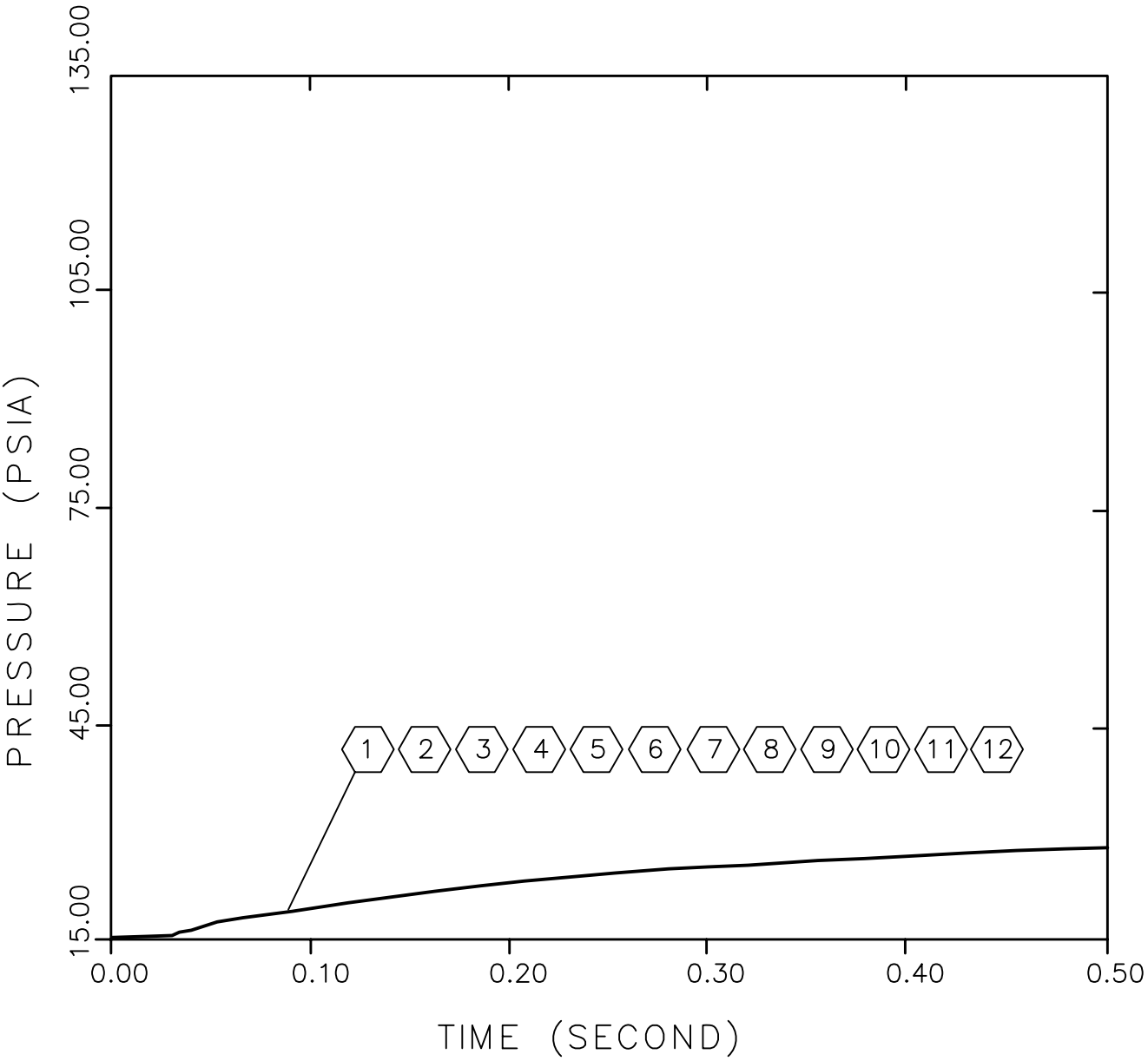

FSAR REV.65

SUSQUEHANNA STEAM ELECTRIC STATION
UNITS 1 & 2
FINAL SAFETY ANALYSIS REPORT

PRESSURE TRANSIENT IN SHIELD ANNULUS FOLLOWING A FEEDWATER LINE BREAK AT THE NOZZLE SAFE END

FIGURE 6A-3G, Rev. 48

AutoCAD: Figure Fsar 6A_3G.dwg

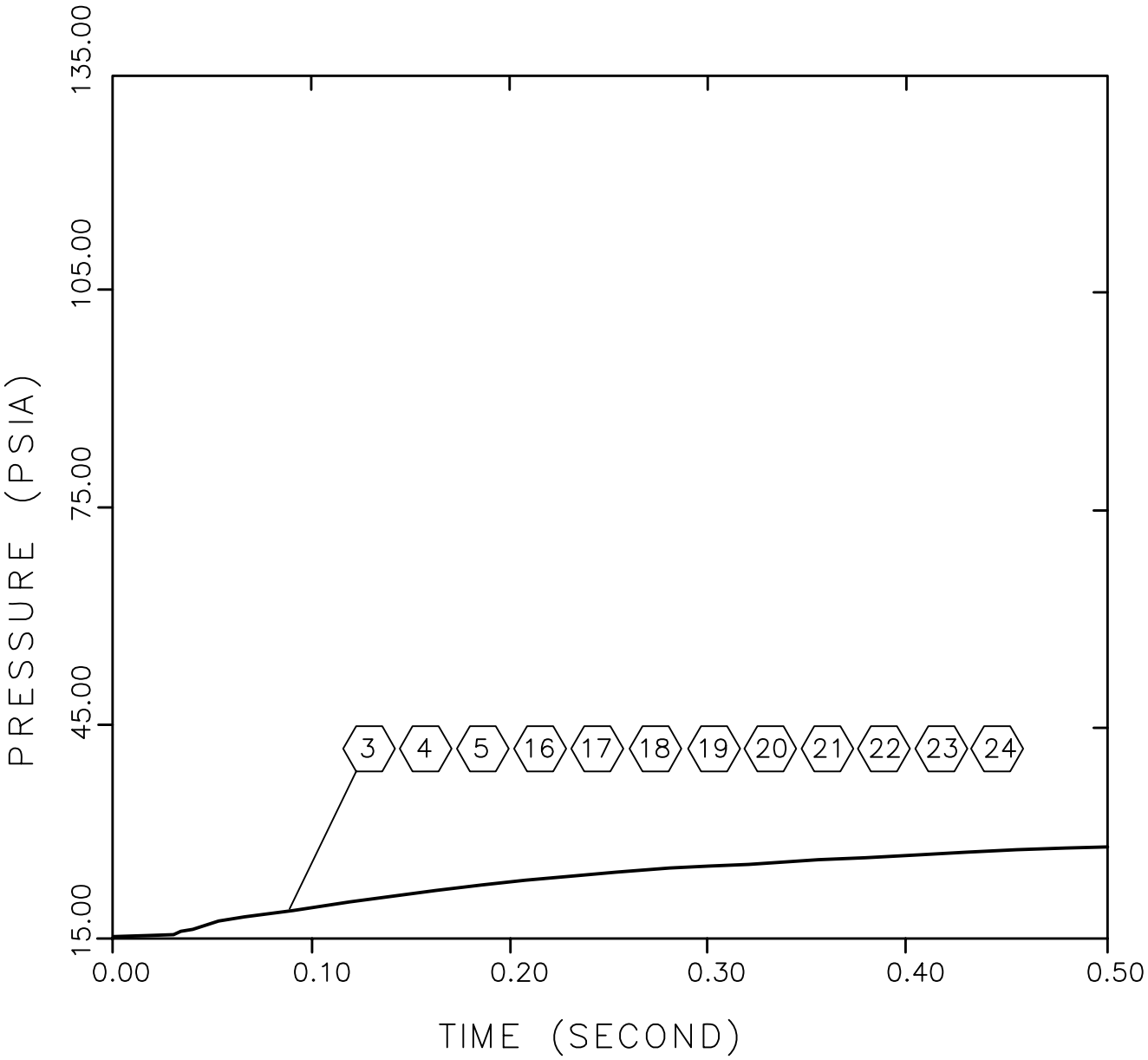

FSAR REV.65

SUSQUEHANNA STEAM ELECTRIC STATION
UNITS 1 & 2
FINAL SAFETY ANALYSIS REPORT

PRESSURE TRANSIENT IN SHIELD ANNULUS FOLLOWING A FEEDWATER LINE BREAK AT THE NOZZLE SAFE END

FIGURE 6A-3H, Rev. 48

AutoCAD: Figure Fsar 6A_3H.dwg

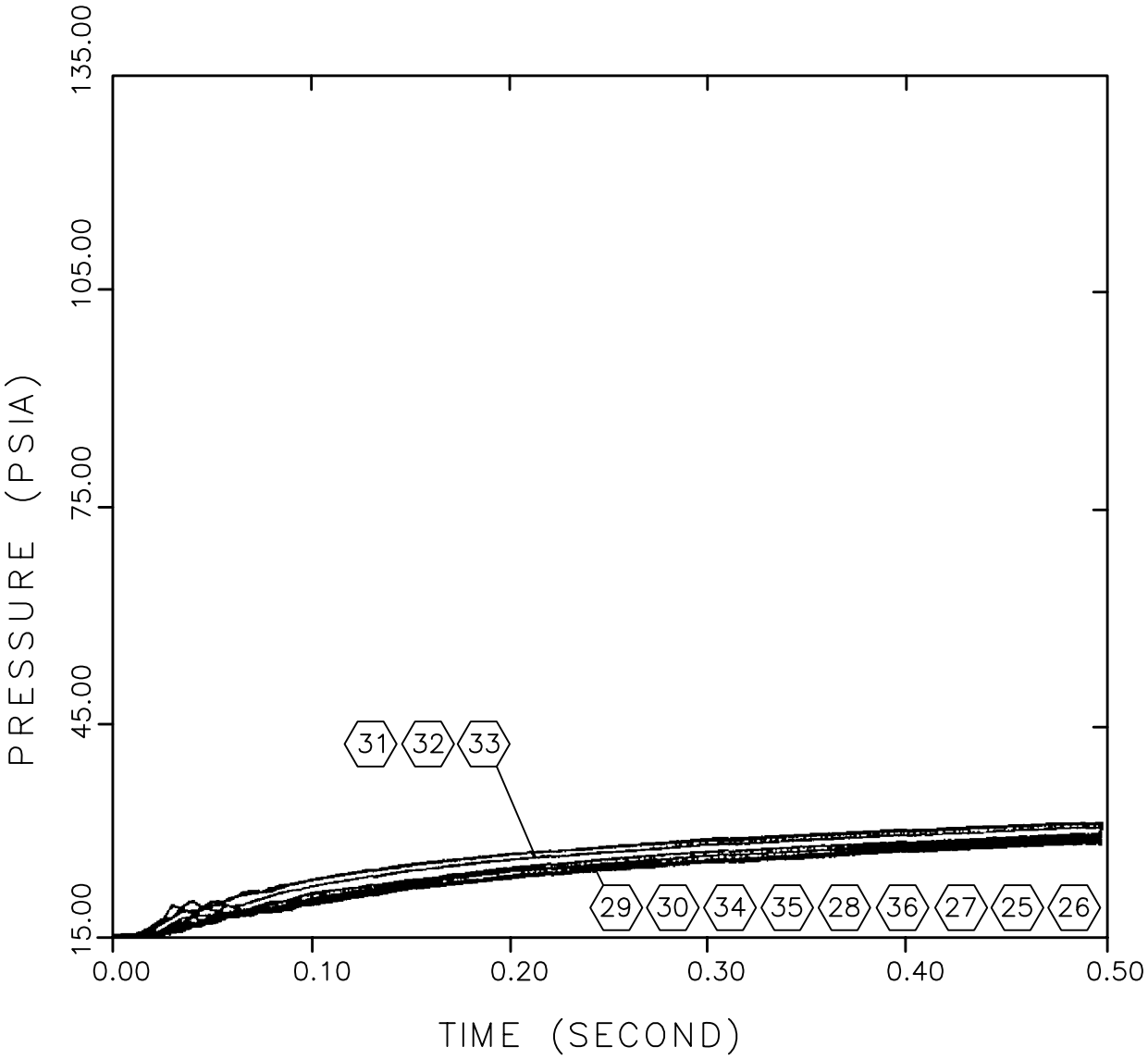

FSAR REV.65

SUSQUEHANNA STEAM ELECTRIC STATION
UNITS 1 & 2
FINAL SAFETY ANALYSIS REPORT

PRESSURE TRANSIENT IN SHIELD ANNULUS FOLLOWING A FEEDWATER LINE BREAK AT THE NOZZLE SAFE END

FIGURE 6A-3I, Rev. 48

AutoCAD: Figure Fsar 6A_3I.dwg

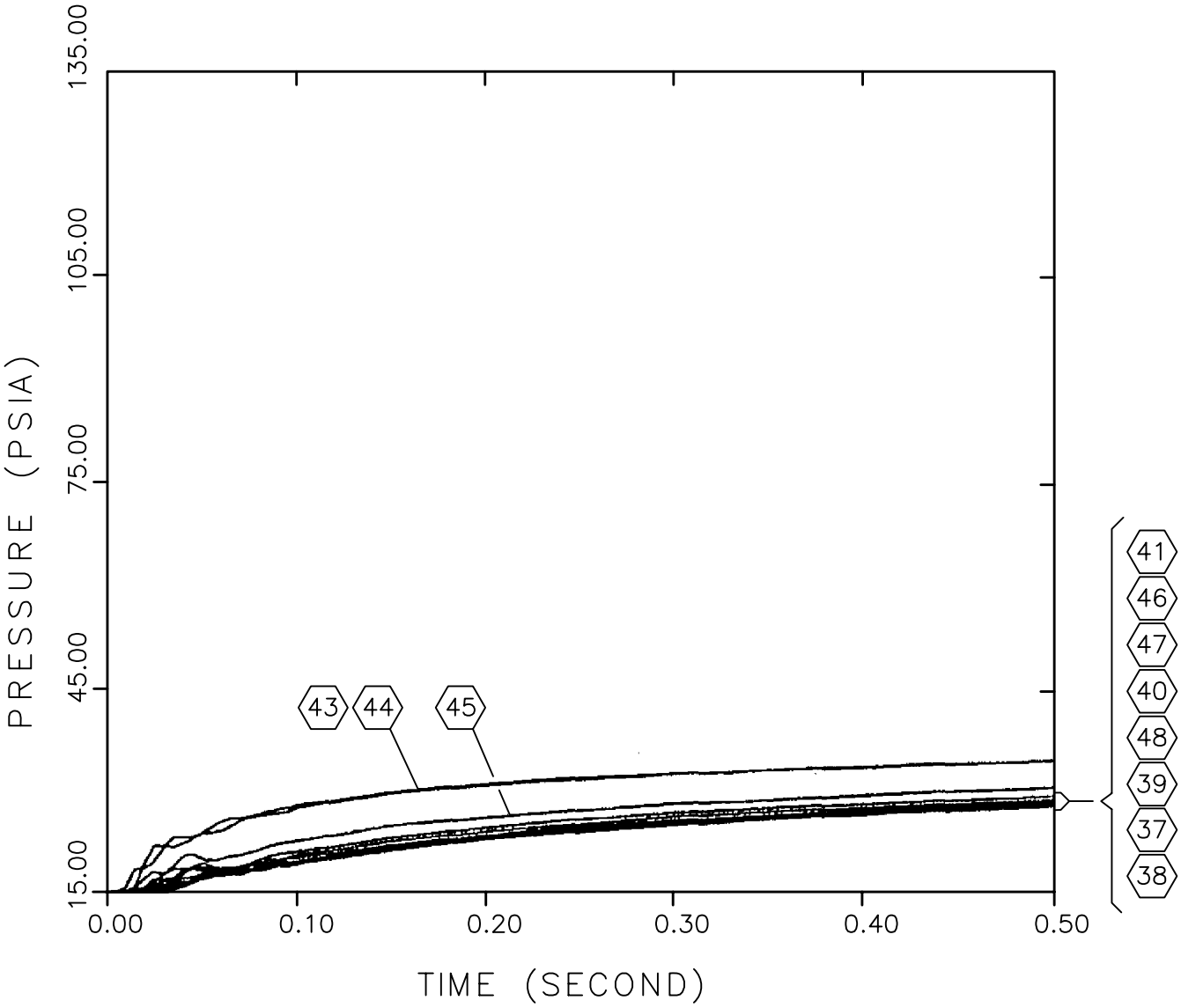

FSAR REV.65

SUSQUEHANNA STEAM ELECTRIC STATION
UNITS 1 & 2
FINAL SAFETY ANALYSIS REPORT

PRESSURE TRANSIENT IN SHIELD
ANNULUS FOLLOWING A FEEDWATER
LINE BREAK AT THE NOZZLE
SAFE END

FIGURE 6A-3J, Rev. 48

AutoCAD: Figure Fsar 6A_3J.dwg

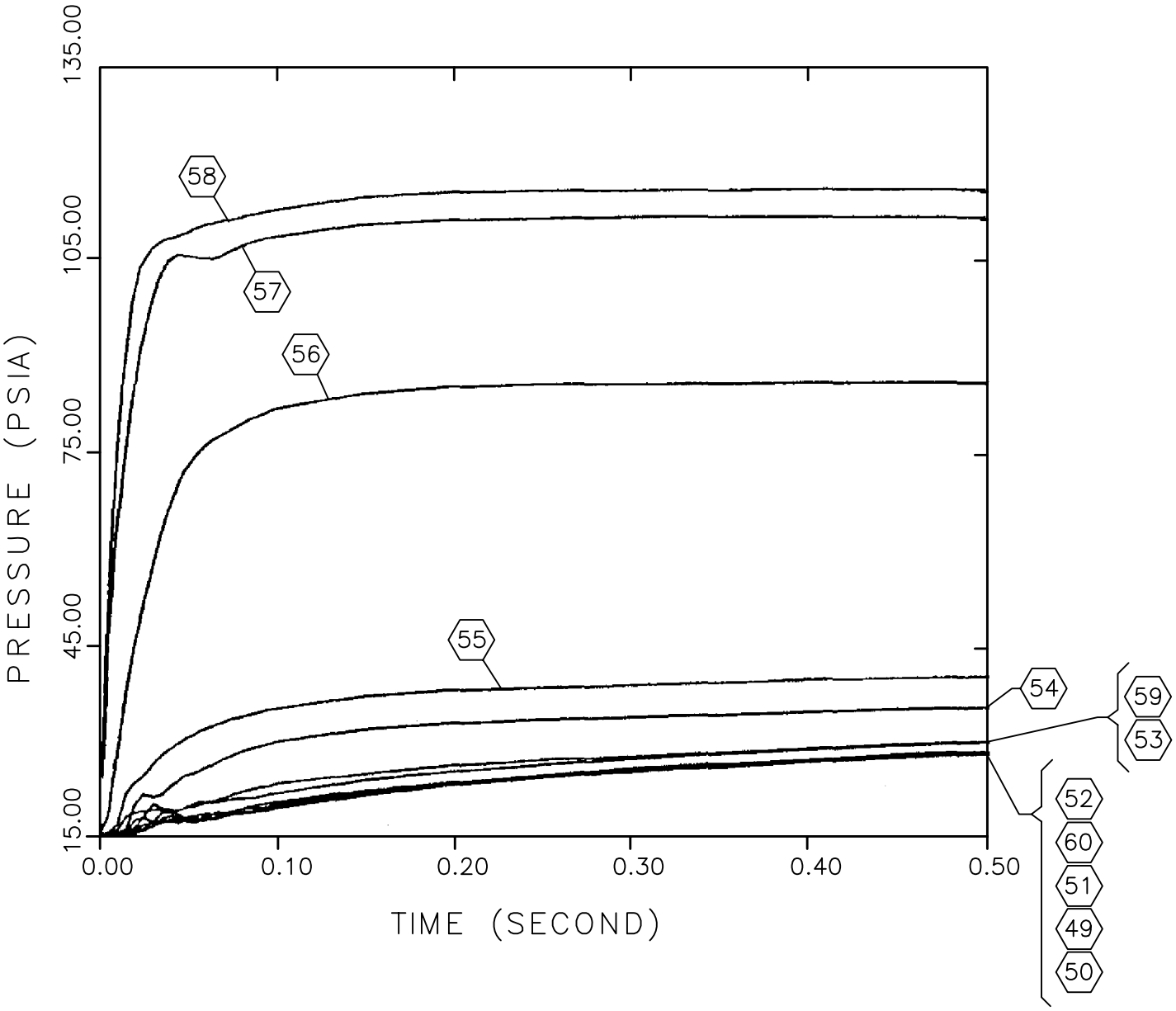

FSAR REV.65

SUSQUEHANNA STEAM ELECTRIC STATION
UNITS 1 & 2
FINAL SAFETY ANALYSIS REPORT

PRESSURE TRANSIENT IN SHIELD ANNULUS FOLLOWING A FEEDWATER LINE BREAK AT THE NOZZLE SAFE END

FIGURE 6A-3K, Rev. 48

AutoCAD: Figure Fsar 6A_3K.dwg

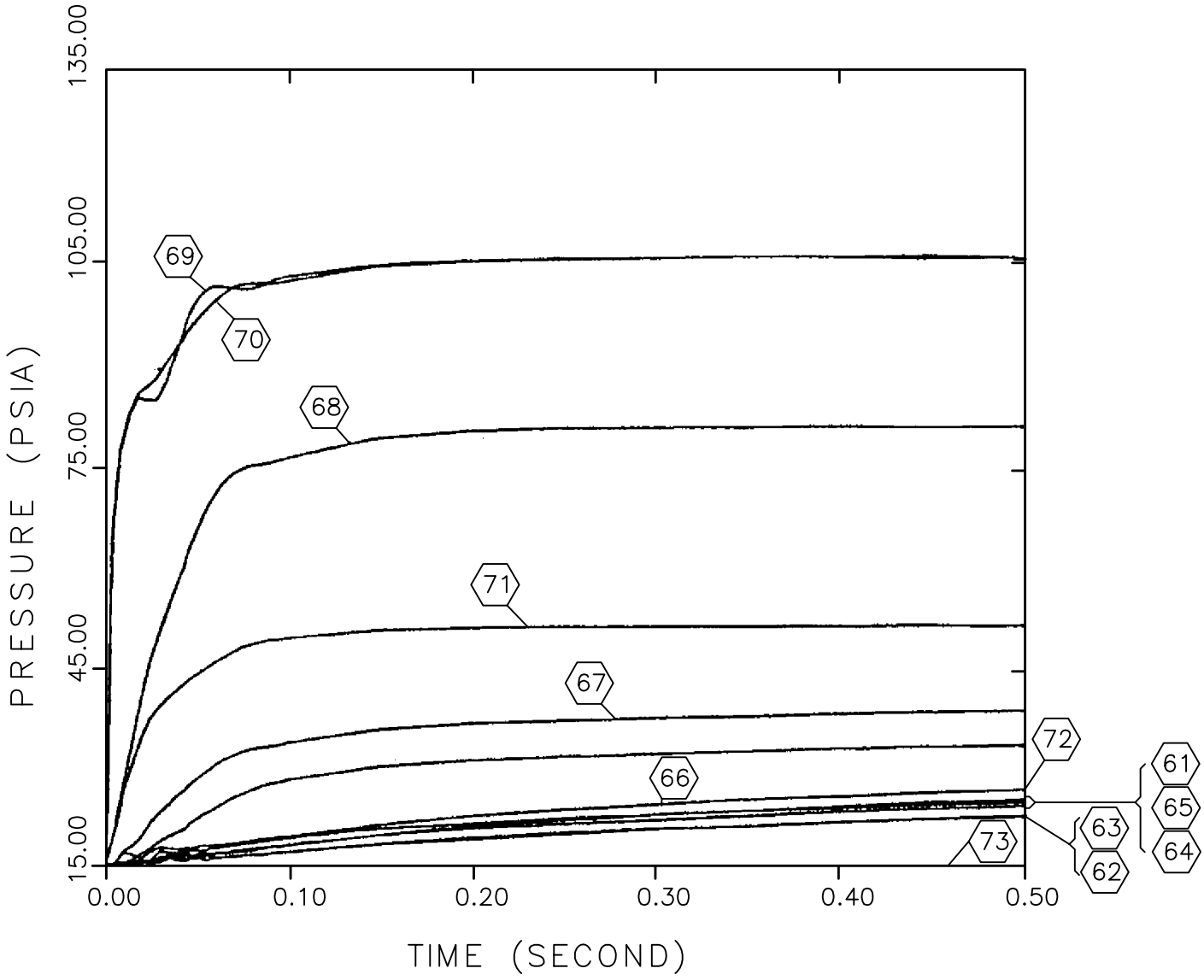

FSAR REV.65

SUSQUEHANNA STEAM ELECTRIC STATION
UNITS 1 & 2
FINAL SAFETY ANALYSIS REPORT

PRESSURE TRANSIENT IN SHIELD ANNULUS FOLLOWING A FEEDWATER LINE BREAK AT THE NOZZLE SAFE END

FIGURE 6A-3L, Rev. 48

AutoCAD: Figure Fsar 6A_3L.dwg

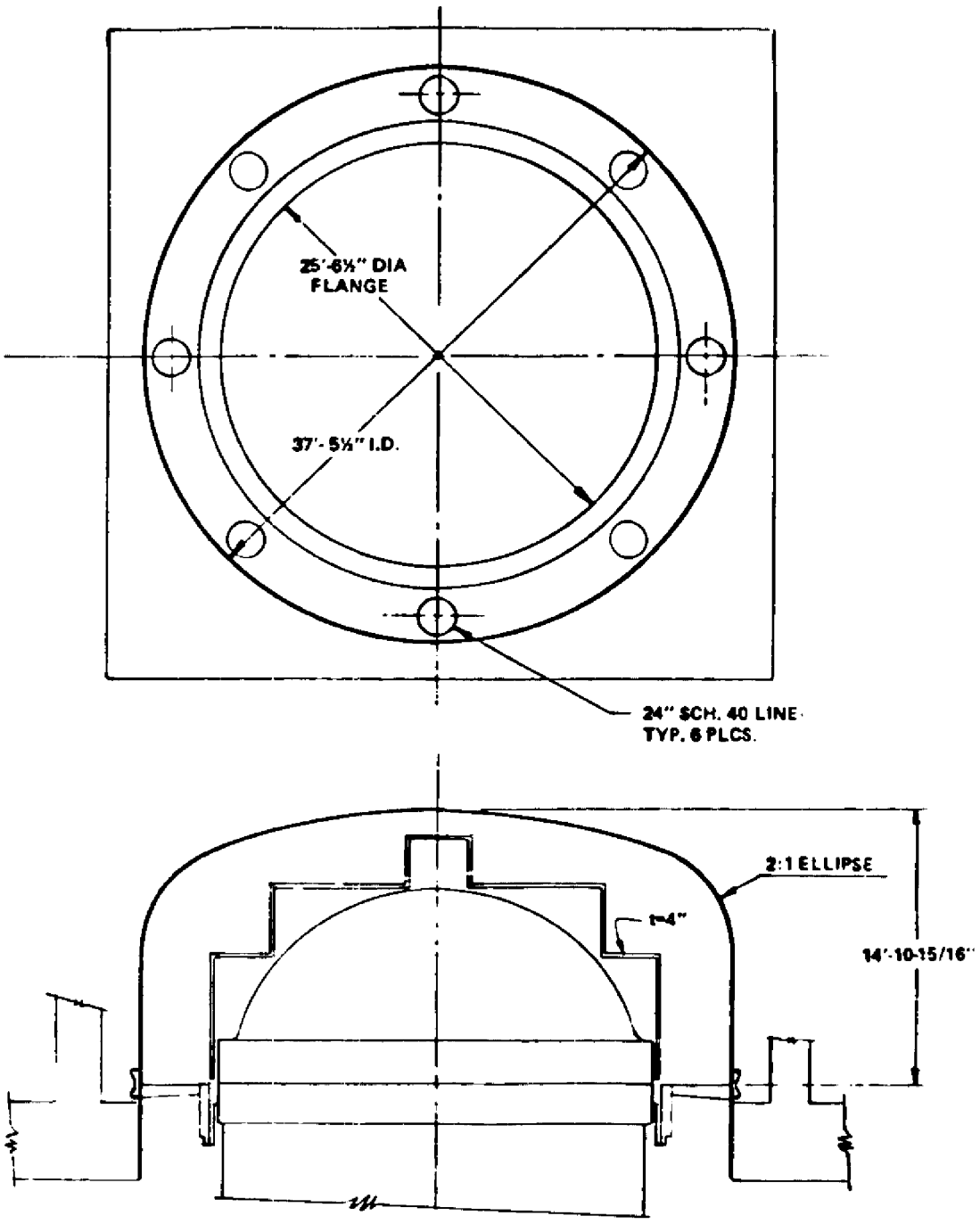

FSAR REV.65

SUSQUEHANNA STEAM ELECTRIC STATION
UNITS 1 & 2
FINAL SAFETY ANALYSIS REPORT

DRYWELL HEAD ARRANGEMENT

FIGURE 6A-4, Rev. 47

AutoCAD: Figure Fsar 6A_4.dwg

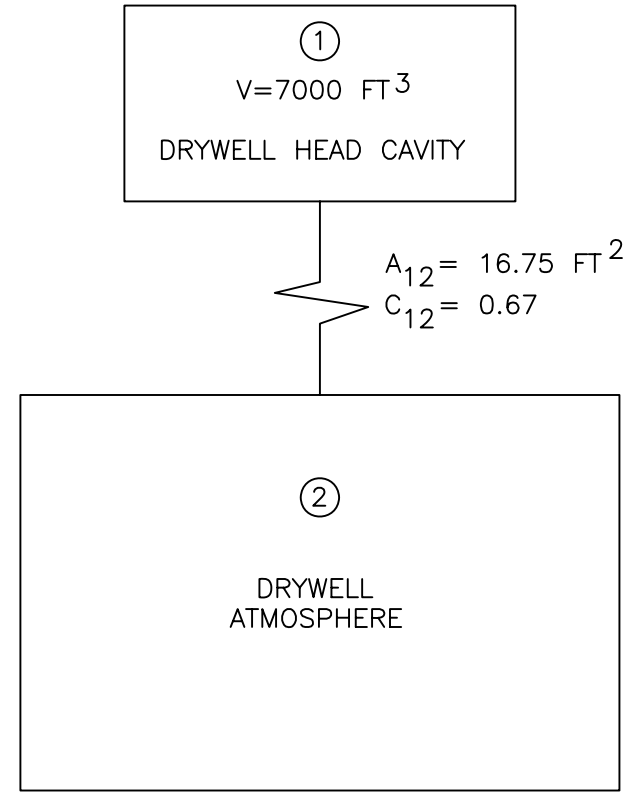

(HEAD SPRAY LINE BREAK IN COMPARTMENT (1))

FSAR REV.65

SUSQUEHANNA STEAM ELECTRIC STATION
UNITS 1 & 2
FINAL SAFETY ANALYSIS REPORT

HEAD SPRAY LINE
BREAK GEOMETRY

FIGURE 6A-5, Rev. 47

AutoCAD: Figure Fsar 6A_5.dwg

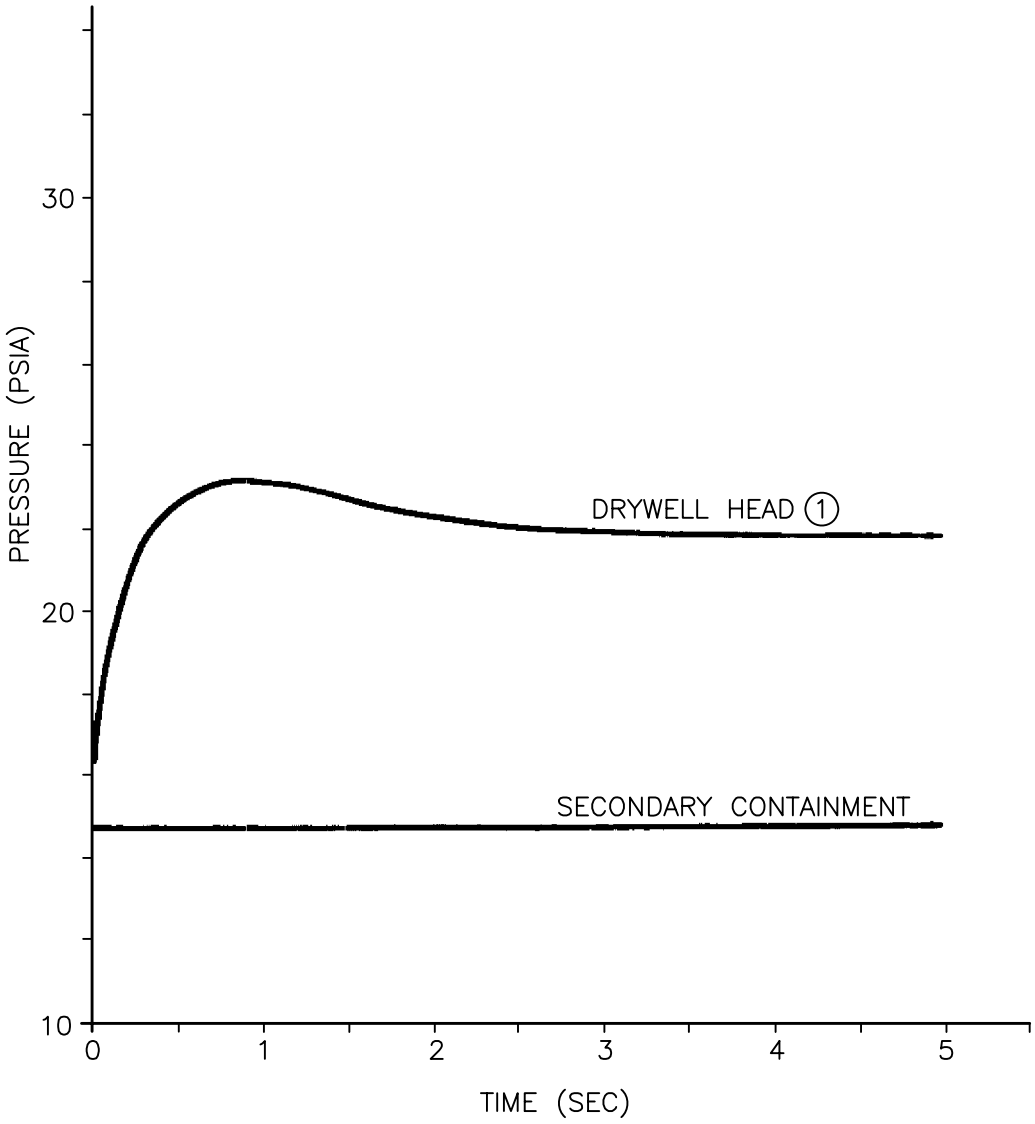

FSAR REV.65

SUSQUEHANNA STEAM ELECTRIC STATION
UNITS 1 & 2
FINAL SAFETY ANALYSIS REPORT

PRESSURE RESPONSE IN THE
DRYWELL HEAD FOR A HEAD
SPRAY LINE BREAK

FIGURE 6A-6, Rev. 47

AutoCAD: Figure Fsar 6A_6.dwg

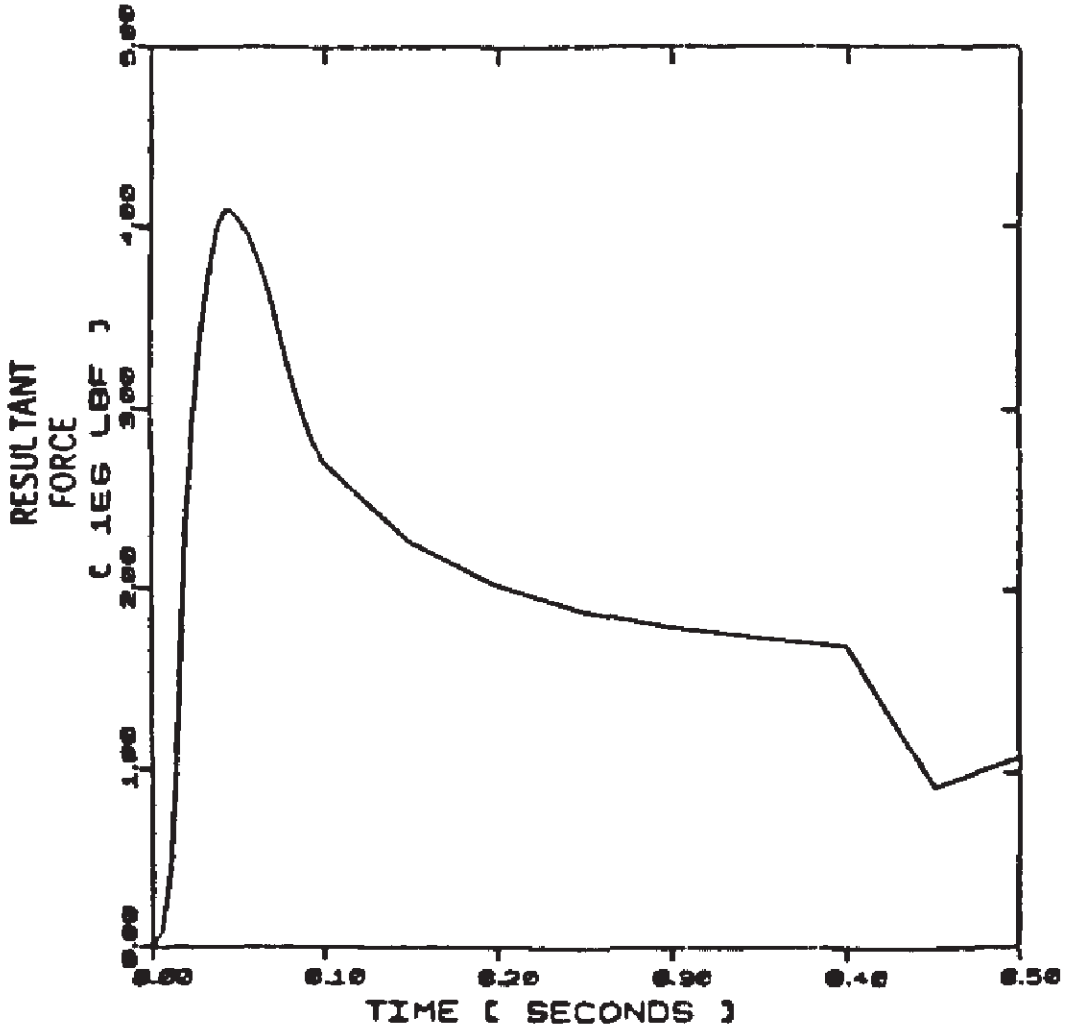

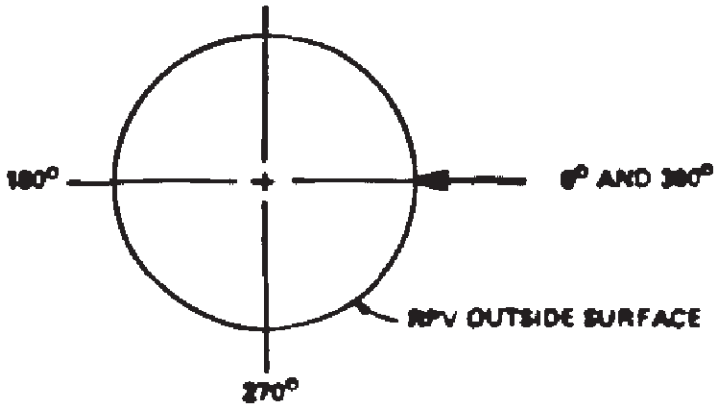

FSAR REV.65

SUSQUEHANNA STEAM ELECTRIC STATION UNITS 1 & 2 FINAL SAFETY ANALYSIS REPORT
FORCE TRANSIENT ON REACTOR PRESSURE VESSEL FOLLOWING A RECIRC. LINE BREAK AT THE NOZZLE SAFE END FIGURE 6A-7, Rev. 47

AutoCAD: Figure Fsar 6A_7.dwg

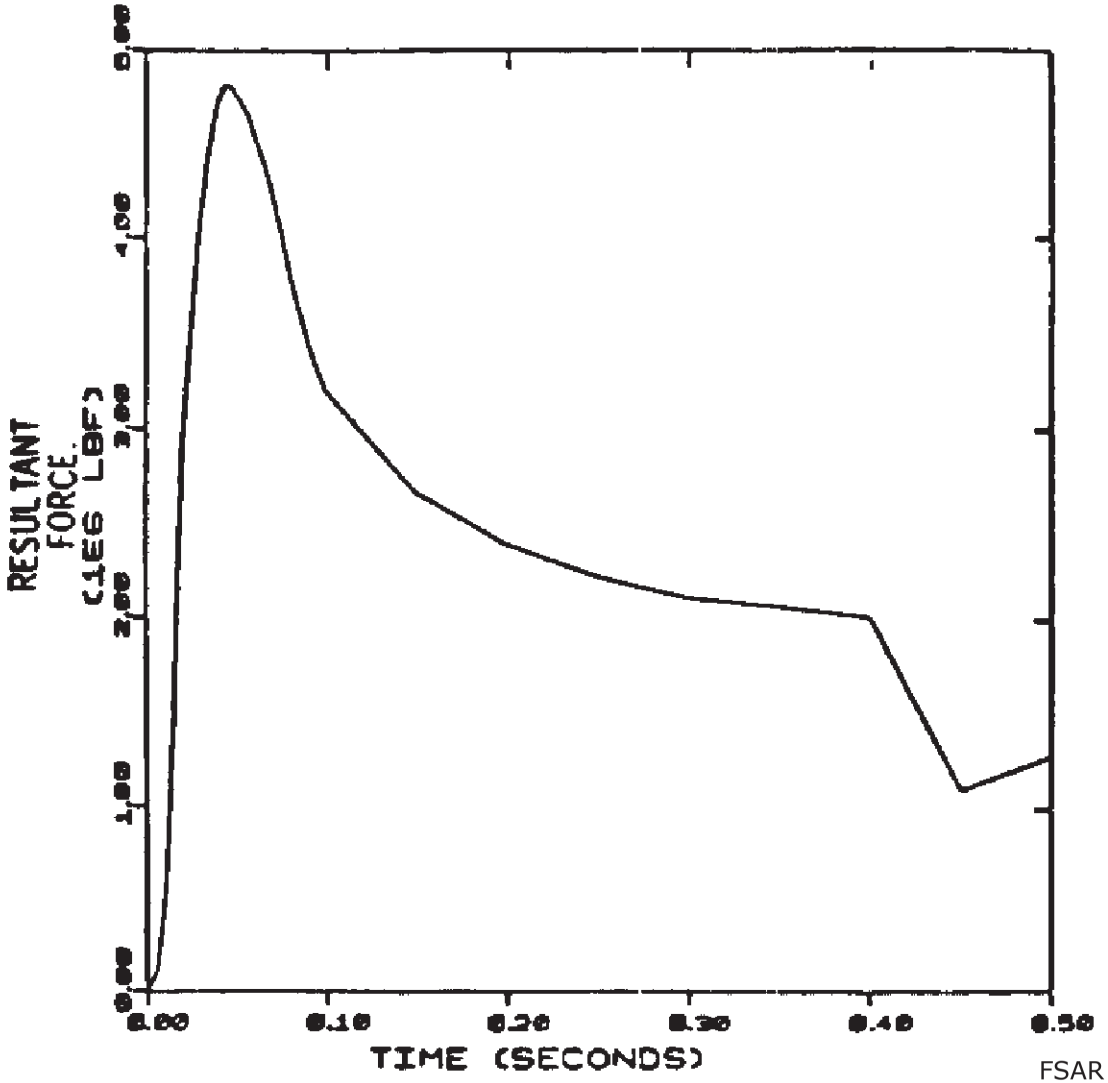

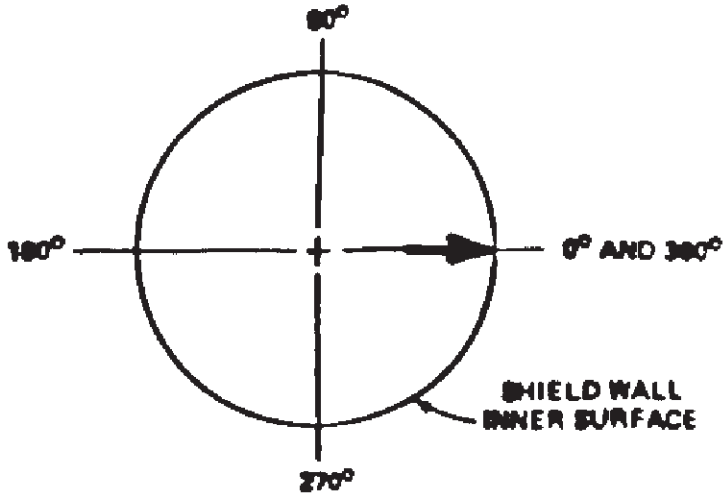

FSAR REV.65

SUSQUEHANNA STEAM ELECTRIC STATION
UNITS 1 & 2
FINAL SAFETY ANALYSIS REPORT

FORCED TRANSIENT ON REACTOR
SHIELD WALL FOLLOWING RECIRC.
LINE BREAK AT THE NOZZLE
SAFE END

FIGURE 6A-8, Rev. 47

AutoCAD: Figure Fsar 6A_8.dwg

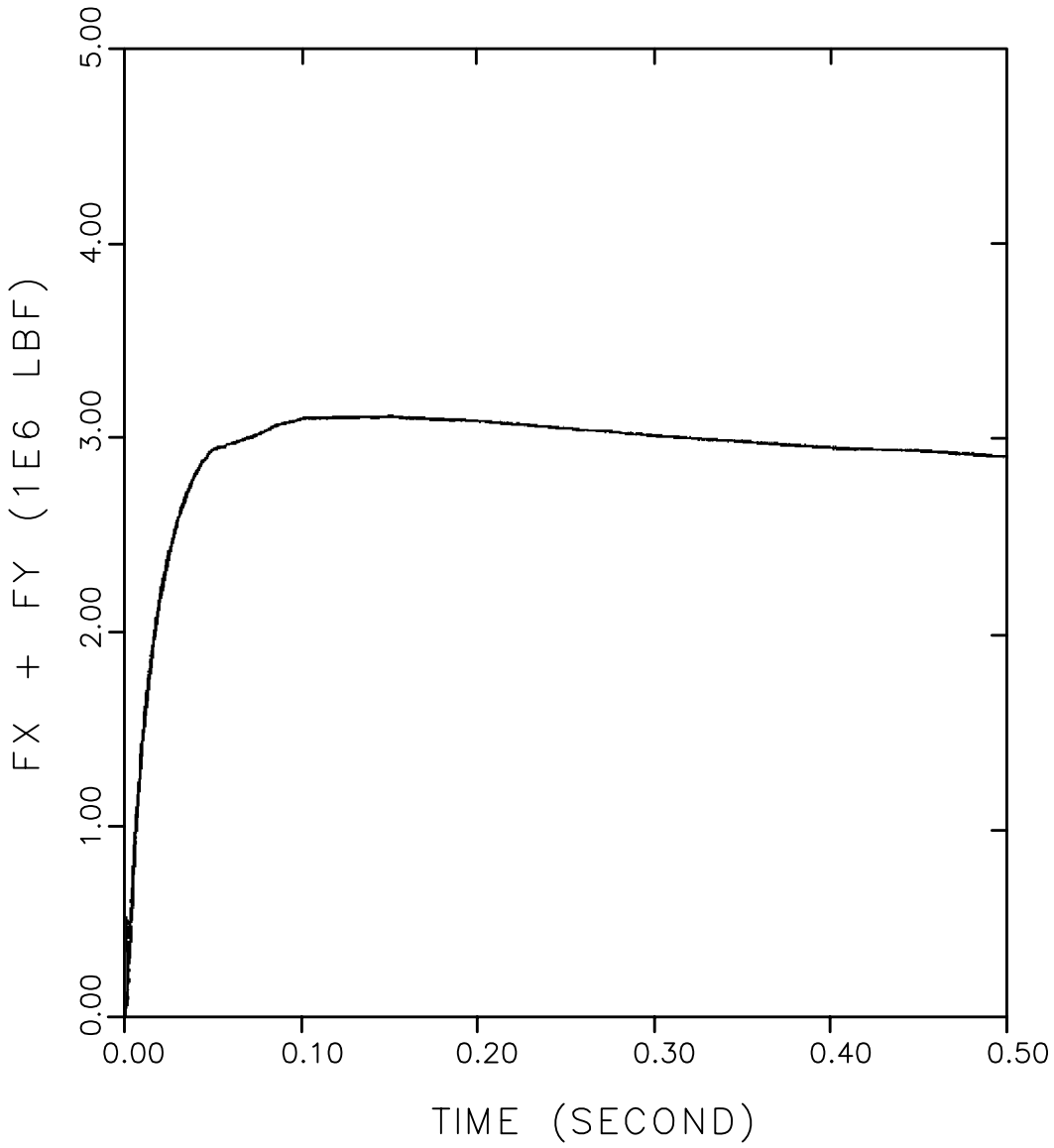

FSAR REV.65

SUSQUEHANNA STEAM ELECTRIC STATION
UNITS 1 & 2
FINAL SAFETY ANALYSIS REPORT

RESULTANT FORCE TRANSIENT ON
RPV FOLLOWING A FEEDWATER
LINE BREAK AT THE NOZZLE

FIGURE 6A-9, Rev. 48

AutoCAD: Figure Fsar 6A_9.dwg

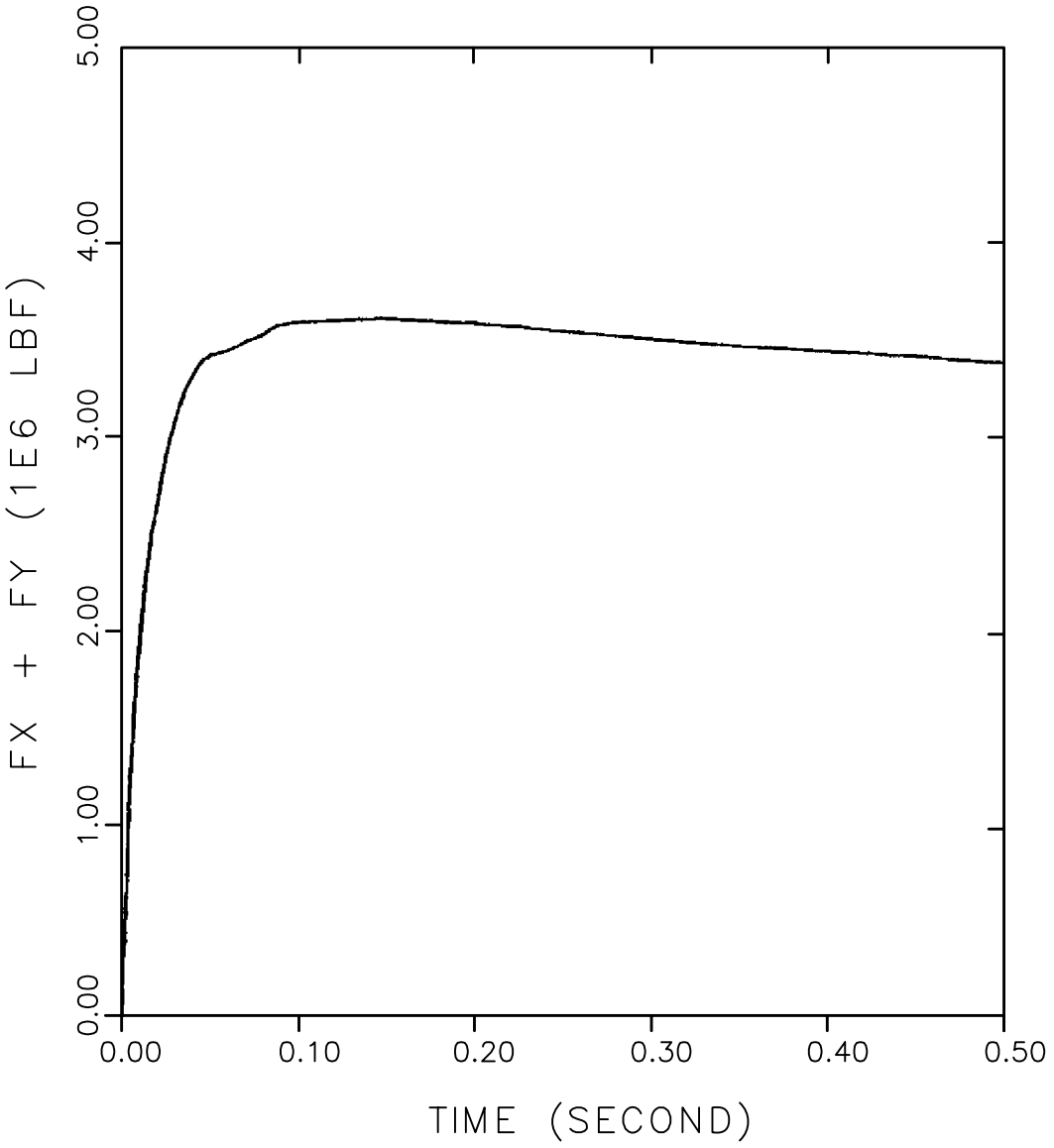

FSAR REV.65

SUSQUEHANNA STEAM ELECTRIC STATION
UNITS 1 & 2
FINAL SAFETY ANALYSIS REPORT

RESULTANT FORCE ON SHIELD
WALL FOLLOWING A FEEDWATER
LINE BREAK AT THE NOZZLE

FIGURE 6A-10, Rev. 48

AutoCAD: Figure Fsar 6A_10.dwg